DESIGN AND ANALYSIS FOR PRECISION MEDICINE SUBGROUP IDENTIFICATION

Crystal T. Nguyen

A dissertation submitted to the faculty of the University of North Carolina at Chapel Hill in partial fulfillment of the requirements for the degree of Doctor of Philosophy in the Department of Biostatistics in the Gillings School of Global Public Health.

Chapel Hill
2019

Approved by:

Michael Kosorok

Eric Bair

Corey Kalbaugh

Anastasia Ivanova

Feng-Chang Lin

ABSTRACT

Crystal T. Nguyen: Design and Analysis for Precision Medicine Subgroup Identification
(Under the direction of Michael Kosorok)

In 2015 President Barack Obama announced the launch of the Precision Medicine Initiative, spurring an out pour of interest into research regarding patient-specific health. Precision medicine is the reproducible research from which health care professionals can provide targeted treatments to their patients. Two objectives in precision medicine include (i) identifying treatment-response subgroups and (ii) identifying disease subgroups. In this manuscript, we will consider a place for traditional study designs in the new age of precision medicine by presenting the machine learning tools and statistical theory necessary to do so.

We begin with a newly proposed method for estimating the individualized treatment regime from crossover studies. This method expands generalized outcome weighted learning into the 2×2 crossover study framework by considering the difference in treatment response as the observed reward and correcting for carryover effects, estimated through regression methods. After, we propose a new technique for identifying disease subgroups by applying hierarchical clustering techniques to what can be interpreted as a set of denoised outcomes. These values are weighted averages of the observed and fitted outcomes, estimated by regressing on a set of features. Finally, we return to identifying treatment-response subgroups, but, in the realm of case-control studies. We again expand on generalized outcome weighted learning in addition to accounting for the difference in the covariate distribution between the selected study sample and the total population. Between this method and electronic health data, advancements for rare and expensive to study diseases may be closer than we think.

To my parents.

At least you can still call me “Doctor.”
But this way I can’t kill anyone. Probably.

ACKNOWLEDGEMENTS

We acknowledge the following NIH institutions for their financial contributions in support of the work presented in this document: NCI P01 CA142538, NIDDK DP3 DK113358, CTSA UL1 TR002489, CTSA UL1 TR001111, NHLBI U24 HL138998, NIH T32 MH106440, and NCMHD P60 MD002254-01.

Writing this document has been my greatest endeavor. Without the assistance of a multitude of faculty, collaborators, and peers, the work presented here would not have been possible. Thank you to Michael Kosorok for being my dissertation advisor and general life mentor. Your guidance and support have been invaluable to the completion of this work. Additionally, thanks to my committee for your time and consideration of this document, and particularly, thanks to Corey Kalbaugh and Eric Bair for your subject matter expertise in epidemiology and clustering, respectively. While our meetings were brief, your contributions have directly affected the end product of Chapters 3 and 4 which were nontrivial to flesh out.

I want to give special thanks to my friends, Michael Lawson, Xiaotong (Phoebe) Jiang, and Nuvan Rathnayaka, for letting me bounce ideas off you (including terrible method acronyms), always being willing to grab a drink with me, and, most of all, putting up with my shenanigans. Warmest of thanks to Anna Kahkoska, my research partner in crime. It has been a privilege to work with you and an honor to be your friend. I am incredibly proud of our work together, and having the emotional support of a fellow woman in research (who is remarkably accomplished!) has been an extraordinary experience. I can never thank you enough for the partnership we have built. Most of all, thanks to Daniel Luckett. This work could not have been completed without your support both professionally and personally. I am forever indebted to you, and I cannot wait to see for what is in store for us next - hopefully not any more degrees.

Lastly, I would like to express my gratitude toward my family. Thanks, Mom and Dad, for teaching me to count, add, and multiply as a child; I'll bet you never thought the fire you sparked then would lead to biostatistics. Thanks to Jon and Nidhi for always offering me your career advice and looking out for my best interests. Last, but certainly not least, thank you, Josh. Words cannot express the thanks I have for the impact you have made on my life. You have supported me through the best of times and the worst of times, and I can't imagine what that journey would have been like without you.

TABLE OF CONTENTS

LIST OF TABLES

LIST OF FIGURES

LIST OF ABBREVIATIONS

ACC/AHA	American College of Cardiology/American Heart Association
ARI	Adjusted Rand Index
BMI	Body Mass Index
BMIz	Body Mass Index z-score
CHF	Coronary Heart Failure
COPD	Chronic Obstructive Pulmonary Disease
EHR	Electronic Health Record
FAME	Food, Adolescents, Mood and Exercise
GOWL	Generalized Outcome Weighted Learning
HbA1c	Hemoglobin A1c
HFLS	High Fiber / Low Sugar
HSLF	High Sugar / Low Fiber
ITR	Individualized Treatment Regime
MSE	Mean Square Error
OWL	Outcome Weighted Learning
PAD	Peripheral Artery Disease
RLT	Reinforcement Learning Trees
RWL	Residual Weighted Learning
T1D	Type 1 Diabetes
VAS	Visual Analog Scale
VQI	Vascular Quality Initiative

CHAPTER 1: INTRODUCTION

Precision medicine is the field of research that aims to personalize treatment based on patient-specific factors in a reproducible way. While the field has been up and coming for some time now, the Precision Medicine Initiative announced by President Obama has led to a surge in precision medicine research. Thanks to great advancements in technology, we now have a plethora of data at our fingertips, but developments in rigorous, peer-reviewed methods for various study aims and designs are still required. It is of particular interest in precision medicine to estimate an optimal individualized treatment regime (ITR) that recommends treatment decisions based on patient characteristics to maximize the mean of some outcome. Many methods have been proposed and used to address this aim, but they primarily focus on randomized clinical trial data and large cohort studies, both of which may be expensive to carry out or difficult to recruit for. Another objective of precision medicine is to identify disease subgroups or phenotypes that are defined by some outcome of interest, but none of the existing methods are well-equipped to handle multivariate outcomes or especially noisy data. In this manuscript, we will introduce three topics for the purpose of subgroup identification in precision medicine that take advantage of easy to implement study designs and/or the pre-existing wealth of data from previous observational studies and electronic health records (EHRs).

Little work has been done in the area of ITR estimation from correlated observations, like those that arise from crossover study designs. Such designs naturally lend themselves to precision medicine, because they allow for observing the response to multiple treatments for each patient. Chapter 2 introduces a method for estimating the optimal ITR using data from a 2×2 crossover study with or without carryover effects. The proposed method is a policy search method, similar

to outcome weighted learning (OWL); however, we take advantage of the crossover design by considering the difference in response under each treatment as the observed reward. We establish Fisher and global consistency, present numerical experiments, and analyze data from a nutritional feeding trial using the proposed method to demonstrate its improved performance compared to standard methods for a parallel study design.

We then shift gears into discussing a new disease subgroup identification method in Chapter 3. In semi-supervised clustering, it may be desirable to produce clusters that are associated with some outcome of interest. However, current methods approach this problem by clustering on the feature space, guided by a univariate outcome. Instead, we propose clustering on a weighted average of the observed outcomes and smoothed outcomes, estimated conditionally on the features, thereby guiding the clusters by these set of features. By doing so, the clusters are more directly informed by the outcomes of interest. In cases where the outcomes are noisy surrogates for some latent class of phenotypes, the proposed method can produce a more accurate clustering than traditional methods. Chapter 3 presents this method alongside simulations and an application to a large cohort study.

The final topic presented in Chapter 4 again deals with estimating the optimal ITR, this time from case-control studies. While there exist a number of methods for optimal ITR estimation from observational studies, such studies are not always feasible for a given disease group. For example, rare diseases require studies with large sample sizes and long follow-up periods, putting the studies at increased risk for patient drop-out and missing data. Thus, case-control studies become an obvious choice, especially in the age of EHRs when such data are so readily available. However, their use in the world of precision medicine is limited because of selection bias. Of course, this is by design: patients with rare diseases are over-sampled into the study. However, the selection bias must be accounted for to maintain a generalizable optimal ITR. The method proposed in Chapter 4 offers a solution by modifying outcome weighted learning with a selection factor, easily estimated with regression methods.

The remainder of this dissertation is organized as follows. A new method for identifying treatment-response subgroups from 2×2 crossover data is presented in Chapter 2. Chapter 3 introduces a novel clustering technique for identifying disease subgroups based on outcomes of interest, guided by a set of features. Identifying treatment-response subgroups is revisited in Chapter 4, but this time from case-control studies. Finally, Chapter 5 provides a brief discussion on future research goals for the topics presented in this manuscript as well as potential future topics. The relevant technical details have been deferred to the corresponding appendices.

CHAPTER 2: ESTIMATING INDIVIDUALIZED TREATMENT REGIMES FROM CROSSOVER DESIGNS

2.1 Introduction

Personalized medicine is the practice of tailoring treatment to account for patient heterogeneity (Chakraborty and Murphy, 2014). Physicians and other health care providers have practiced personalized medicine by adjusting doses or prescriptions based on a patient's medical history or demographics for centuries (Ashley, 2015; Zhao and Zeng, 2013). Precision medicine is an emerging field that aims to support personalized medicine decisions with reproducible research (Collins and Varmus, 2015). Such research is imperative, particularly when diseases are expressed with great heterogeneity across patients. A topic of interest in precision medicine is the individualized treatment regime (ITR): a set of decision rules for one or more decision time points that can be used to assign patients to treatment tailored by their patient-specific factors (Lavori and Dawson, 2014; Moodie et al., 2007; Petersen et al., 2007). One objective in precision medicine is to estimate the optimal ITR, or the ITR that maximizes the mean of some desirable outcome (Kosorok and Moodie, 2015; Laber et al., 2014). Crossover clinical trials are uniquely suited to precision medicine, because they allow for observing responses to multiple treatments for each patient. This paper introduces a method to estimate optimal ITRs using data from a crossover study by extending generalized outcome weighted learning (GOWL) (Chen et al., 2018) to deal with correlated outcomes.

In a crossover study, patients are randomized to a sequence of treatments rather than a single treatment. Thus, multiple outcomes are observed, one per subject from each treatment period, and each subject acts as his or her own control for reduced between-subject variability (Machin

and Fayers, 2010; Turner, 2010; Wellek and Blettner, 2012). Therefore, crossover designs naturally lend themselves to precision medicine; estimating the optimal ITR from a crossover design can utilize all counterfactual outcomes. In contrast, estimating the optimal ITR from traditional parallel group designs, where patients are assigned to a single treatment, can only utilize the subset of counterfactual outcomes that are observed.

There have been many developments in machine learning methods for answering precision medicine questions from parallel study designs. For example, Qian and Murphy (2011) indirectly estimate the decision rule using L_1 penalized least squares; Zhang et al. (2012a) maximize a doubly robust augmented inverse probability weighted estimator for the population mean outcome; Athey and Wager (2017) maximize a doubly robust score that may take into account instrumental variables; Kallus (2018) employs a weighting algorithm similar to inverse probability weighting but minimize the worst case mean square error; Laber and Zhao (2015) propose the use of decision trees, which prove to be both flexible and easily interpretable; Zhao et al. (2012), Zhang et al. (2012b), Zhou et al. (2017), and Chen et al. (2018) directly estimate the decision rule by viewing the problem from a weighted classification standpoint.

However, little work has been done to develop precision medicine methods that handle correlated observations in the single-stage decision setting such as those that arise from crossover designs. (Kulasekera and Siriwardhana, 2018) propose a weighted ranking algorithm to estimate a decision rule that maximizes either the expected outcome or the probability of selecting the best treatment, but they assume that there are no carryover effects present. Because the intended effect of the washout period can be difficult to achieve in practice (Wellek and Blettner, 2012), it is imperative that methods for crossover designs can be applied when carryover effects are present. In this paper, we show that the difference in response to two treatments from a 2×2 crossover trial can be used as the reward in the GOWL objective function to estimate an optimal ITR. We introduce a plug-in estimator that can be used with the proposed method to account for carryover effects. Additionally, we show that using a crossover design with the proposed method results in

improvements in misclassification rate and estimated value when compared to standard methods for a parallel design at the same sample size.

As a clinical example, consider nutritional recommendations surrounding the intake of dietary fiber for the purpose of weight loss. Although increased fiber is recommended across the population for a myriad of health benefits (Anderson et al., 1994, 2009; Marlett et al., 2002; US Department of Agriculture, 2010), evidence of the impact of the consumption of dietary fiber for improved satiety and reduction in body weight is mixed (Halliday et al., 2018; Slavin, 2005). Heterogeneity in response to dietary fiber may be leveraged to develop targeted fiber interventions to promote feelings of satiety. We use data from a crossover study in which Hispanic and African American adolescents who are overweight and obese were fed breakfast and lunch under a typical western high sugar diet and a high fiber diet. From these data, we estimate a decision rule with which clinical care providers can input patient characteristics, including demographics and clinical measures, and receive a recommendation to maximize the change in measures of perceived satiety from before breakfast to after lunch. This type of analysis could be useful in identifying a subgroup of at-risk adolescents for which targeting specific dietary recommendations is expected to lead to an increase in patient-reported satiety, helping to decrease caloric intake in a population with great clinical need for effective weight loss strategies.

The rest of this paper is organized as follows. In Section 2.2, we review outcome weighted learning (OWL) (Zhao et al., 2012) and present the proposed method for estimating an optimal ITR from a crossover study regardless of the presence of carryover effects. Section 2.3 establishes Fisher and global consistency. Section 2.4 demonstrates the performance of the proposed method in simulation studies, with results on misclassification rate and estimated value. Section 2.5 displays an analysis of data from a feeding trial with overweight and obese Latino and African American adolescents, and we conclude with a discussion in Section 2.6.

2.2 Methodology

In this section, we provide a brief overview of existing methods for estimating the optimal ITR using weighted classification. We then provide the justification and means to implement our proposed method, which we will from here refer to as "crossover GOWL."

2.2.1 Existing Methods

Consider a parallel, two-arm clinical trial in which we have i.i.d. observations $(\boldsymbol{X}_i, A_i, Y_i)$ for $i = 1, \ldots, n$, where $A \in \mathcal{A} = \{-1, 1\}$ is binary treatment assignment, $\boldsymbol{X} \in \mathcal{X}$ is a p-dimensional vector of covariates, and $Y \in \mathbb{R}$ is a reward, bounded by $M_0 < \infty$, for which greater values are desired. Assume that Y is of the form

$$Y = \mu(\boldsymbol{X}) + Ac(\boldsymbol{X}) + \epsilon,$$

where $\mu(\boldsymbol{X})$ is the main effect of the covariates, $c(\boldsymbol{X})$ is the treatment-covariate interaction, and ϵ has mean 0 and variance σ_ϵ^2. Denote $Y^*(a)$ as the counterfactual outcome under treatment a. We then make three causal assumptions (Rubin, 1978) to connect the counterfactual outcomes to the observed data: $P(A = a|\boldsymbol{X}) > 0$ with probability 1, $\{Y^*(1), Y^*(-1)\}$ is independent of A conditional on $\boldsymbol{X}$, and $Y = Y^*(a)$. These are known as positivity, conditional exchangeability, and consistency, respectively.

An ITR, D, comes from the set of all functions, $\mathcal{D}$, that map the covariate space, $\mathcal{X}$, to the treatment space, $\mathcal{A}$. Our objective is to estimate the optimal ITR, denoted D_0, which maximizes the value function (Qian and Murphy, 2011),

$$\mathcal{V}(D) = E\left[\frac{Y1\{A = D(\boldsymbol{X})\}}{P(A|\boldsymbol{X})}\right], \tag{2.1}$$

where $P(A|\boldsymbol{X}) = \Pr(A = a|\boldsymbol{X} = \boldsymbol{x})$ is the propensity score for treatment. Equivalently, D_0 may be defined as

$$D_0 = \underset{D \in \mathcal{D}}{\operatorname{argmin}} E\left[\frac{Y1\{A \neq D(\boldsymbol{X})\}}{P(A|\boldsymbol{X})}\right]. \tag{2.2}$$

Zhao et al. (2012) propose OWL to solve this problem: each misclassified observation is weighted by its observed outcome, Y, and the hinge loss is used to bring the problem into the support vector machine framework (Cortes and Vapnik, 1995). Unfortunately, OWL assumes Y is nonnegative; when negative values are observed, OWL shifts all outcomes to be nonnegative, since (2.2) is invariant to such a transformation. The objective function in OWL, however, does not have this property. Therefore, the estimated decision function in OWL depends on the chosen shift in the outcomes. Chen et al. (2018) propose GOWL, an extension of OWL, which handles negative rewards by modifying the hinge loss to be piecewise and weighting the misclassified observations by $|Y|$. With GOWL, there is no need to shift rewards.

However, neither Zhao et al. (2012) nor Chen et al. (2018) considered correlated outcomes, such as those that arise from a crossover design setting. We now introduce crossover GOWL, a method that combines the observed treatment response difference with GOWL to estimate the optimal ITR from 2×2 crossover data.

2.2.2 Crossover Generalized Outcome Weighted Learning

In a crossover design, patients are randomly assigned to a sequence of treatments rather than a single treatment. For the 2×2 design, patients are randomized to receive either the $(-1, 1)$ or the $(1, -1)$ sequence, with some prespecified washout period between treatments. The washout period is a break between treatments which serves to remove any carryover effects, i.e., residual effects remaining from a previous treatment at the start of the next treatment. Keeping most of the notation from before, we now introduce sequential treatments and outcomes A_k and Y_k for periods $k = 1, 2$, respectively. Thus, Y_k is the observed outcome after receiving treatment A_k in

period k. Furthermore, we assume the model

$$Y_k = \mu(\boldsymbol{X}) + A_k c(\boldsymbol{X}) + \delta_{A_1}(\boldsymbol{X})\, 1\{k = 2\} + \epsilon_k$$

where $\boldsymbol{\epsilon} = (\epsilon_1, \epsilon_2)^\top$ has mean $\mathbf{0}$ and a positive definite covariance matrix, Σ_ϵ, and $\delta_{A_1}(\boldsymbol{X})$ is the carryover effect which may depend on A_1 and $\boldsymbol{X}$. Note that in a 2×2 crossover study, the period effects, or temporal effects, are nonseparable from the carryover effects (Fleiss, 1989), so $\delta_{A_1}(\boldsymbol{X})$ encompasses both period and carryover effects.

Let $R = Y_1 - [Y_2 - \delta_{A_1}(\boldsymbol{X})]$. Given the observed data $(\boldsymbol{X}, A_1, \boldsymbol{Y})$, where $\boldsymbol{Y} = (Y_1, Y_2)$, we propose the following as a substitute for the value function to be maximized:

$$E\left[\frac{R}{P(A_1|\boldsymbol{X})} 1\{A_1 = D(\boldsymbol{X})\}\right], \tag{2.3}$$

where $P(A_1|\boldsymbol{X})$ is the probability of being assigned to the sequence $(A_1, -A_1)$ conditional on $\boldsymbol{X}$. Under Lemma 2.1, maximizing (2.3) is equivalent to minimizing (2.2); the proof is left to Appendix A

Lemma 2.1. *Under the given assumptions,*

$$D_0 = \underset{D \in D}{\operatorname{argmin}}\, E\left[\frac{R}{P(A_1|\boldsymbol{X})} 1\{A_1 \neq D(\boldsymbol{X})\}\right].$$

Following (2.3), we use an approach similar to GOWL but weight misclassified observations by the treatment response difference, and we minimize the objective function (2.4) for f in $\mathcal{F}$, a class of functions, e.g., a reproducing kernel Hilbert space. Let $\psi(u, v) = \max\{1 - \operatorname{sign}(u)v, 0\}$, λ_n be a tuning parameter, and $||f||$ be the L_2 norm of f. For details on solving the optimization problem in (2.4), we defer to Chen et al. (2018) and Kimeldorf and Wahba (1970).

$$\underset{f \in \mathcal{F}}{\operatorname{argmin}} \frac{1}{n} \sum_{i=1}^{n} \frac{|R_i|}{P(A_{i,1}|\boldsymbol{X}_i)} \psi\{R_i, A_{i,1} f(\boldsymbol{X}_i)\} + \lambda_n ||f||^2, \tag{2.4}$$

In practice, the true value of $\delta_{A_1}(\boldsymbol{X})$ is unknown. In traditional analyses, we are concerned with testing the null hypothesis that $\delta_{-1}(\boldsymbol{X}) = \delta_1(\boldsymbol{X})$. Here, we are instead interested in whether or not either treatment has a nonzero carryover effect. Investigators may determine whether carryover effects are present any number of ways, including two-sample t-tests for the null hypotheses $H_{0,1}$: $E[\delta_1(\boldsymbol{X})] = 0$ and $H_{0,-1}$: $E[\delta_{-1}(\boldsymbol{X})] = 0$ by comparing mean responses to each treatment at each time point. An estimator for $\delta_{A_1}(\boldsymbol{X})$, denoted $\widehat{\delta}_{A_1}(\boldsymbol{X})$, can be computed using Algorithm 2.1.

Algorithm 2.1: Estimating $\delta_{A_1}(\boldsymbol{X})$
1. Estimate $g(\boldsymbol{x}, a_1) = E[Y_1 \vert \boldsymbol{X} = \boldsymbol{x}, A_1 = a_1]$ by regressing Y_1 on $\boldsymbol{X}$ and A_1.
2. Set $\widehat{Y}_2 = \widehat{g}(\boldsymbol{X}, A_2)$.
3. Estimate $\delta_{A_1}(\boldsymbol{X})$ by regressing $Y_2 - \widehat{Y}_2$ on $\boldsymbol{X}$ and A_1.

In short, one model is fit to predict what would have been observed in period 2 in the absence of carryover effects, and another model is fit to predict the residual from the first model. While any regression technique may be used here, we use reinforcement learning trees (RLT) in our implementation. RLT is a nonparametric tree-based machine learning method that considers future splits or branches in the model when determining the best split at any node (Zhu et al., 2015).

We can now correct the observed reward with the estimated carryover effects. Letting $\widehat{R} = Y_1 - \left[Y_2 - \widehat{\delta}_{A_{i,1}}(\boldsymbol{X})\right]$, the estimated decision function is

$$\widehat{f}_n^* = \underset{f \in \mathcal{F}}{\operatorname{argmin}} \frac{1}{n} \sum_{i=1}^{n} \frac{|\widehat{R}_i|}{P(A_{i,1}|\boldsymbol{X}_i)} \psi \left\{ \widehat{R}_i, A_{i,1} f(\boldsymbol{X}_i) \right\} + \lambda_n ||f||^2, \tag{2.5}$$

and our proposed estimator of the optimal ITR is $\widehat{D}^*(\boldsymbol{X}) = \operatorname{sign}\left\{ \widehat{f}_n^*(\boldsymbol{X}) \right\}$, where

$$D^* = \underset{D \in \mathcal{D}}{\operatorname{argmax}} \; E\left[\frac{|R|}{P(A_1|\boldsymbol{X})} \psi\{R, A_1 f(\boldsymbol{X})\} \right].$$

2.3 Theoretical Results

In this section, we establish both Fisher and global consistency. First, define the risk under 0-1 loss to be $\mathcal{R}(f) = E[Y\ 1\{A \neq \text{sign}[f(\boldsymbol{X})]\}/P(A|\boldsymbol{X})]$. The risk under the modified loss function with the reward defined as the treatment response difference is then

$$\mathcal{R}_\psi(f) = E\left[\frac{|\widehat{R}|}{P(A_1|\boldsymbol{X})}\psi\left\{\widehat{R}, A_1 f(\boldsymbol{X})\right\}\right].$$

Let $f^*(\boldsymbol{X}) = \text{argmin}_{f\in\mathcal{F}}\,\mathcal{R}_\psi(f)$, so that the corresponding ITR under the modified loss for the treatment response difference is $D^*(\boldsymbol{X}) = \text{sign}\{f^*(\boldsymbol{X})\}$. Under Theorem 2.1, Fisher consistency for $D^*(\boldsymbol{X})$ is derived.

Theorem 2.1. *Under the given assumptions,* $D^*(\boldsymbol{X}) = D_0(\boldsymbol{X})$.

Consider that $\mathcal{F} = \{k(\cdot, \boldsymbol{x}) : \boldsymbol{x} \in \mathcal{X}\}$ for some kernel function k, and let $\overline{\mathcal{F}}$ be the closure of $\mathcal{F}$. Define f_0 to be the minimizer over all functions f for $\mathcal{R}(f)$, and define f_0^* to be the same for $\mathcal{R}_\psi(f)$.

Theorem 2.2. *Let* $\lambda_n > 0$ *be a sequence such that* $\lambda_n \to 0$ *and* $\lambda_n n \to \infty$ *with probability going to 1 as* $n \to \infty$. *Assume* $\exists\, M_1 < \infty$ *such that* $P\left(|\widehat{\delta}_{A_1}(\boldsymbol{X})| < M_1\right) \to 1$ *as* $n \to \infty$ *and* $|\delta_{A_1}(\boldsymbol{X})| < M_1$ *almost surely. If* $\mathbb{P}\left[1\{\text{sign}[\widehat{R}] \neq \text{sign}[R]\}\right] = o_P(\lambda_n)$, *then, for any distribution* P *of* $(\boldsymbol{X}, A_1, \boldsymbol{Y})$, $\lim_{n\to\infty}\mathcal{R}_\psi(\widehat{f}_n^*) \to_P \mathcal{R}_\psi\left(f^*\right)$. *Furthermore, if* $f_0^* \in \overline{\mathcal{F}}$,

$$\lim_{n\to\infty}\mathcal{R}(\widehat{f}_n^*) \to_P \mathcal{R}\left(f_0\right).$$

Derivation of Theorems 2.1 and 2.2 may be found in Appendix A.

2.4 Simulation Studies

To illustrate the benefits of using crossover GOWL, we present simulation studies with comparisons to standard methods. The standard methods are impelemented on period 1 data alone, resembling analysis on a parallel design. Simulated data sets were generated as follows. The covariates, $\boldsymbol{X}_1, \ldots, \boldsymbol{X}_{50}$, are i.i.d. variables drawn from a $U(-1, 1)$ distribution. Subjects were randomized to treatment -1 or 1 for the parallel design or to sequence $(-1, 1)$ or $(1, -1)$ for the crossover design with equal probability. The response for the parallel design, Y, is normally distributed with a mean of $\mu(\boldsymbol{X}) + c(\boldsymbol{X})A$ and a variance of 1. For the crossover design, responses were simulated per the model $Y_k = \mu(\boldsymbol{X}) + A_k c(\boldsymbol{X}) + \delta_{A_1}(\boldsymbol{X})\, 1\{k = 2\} + \epsilon_k$, for $k = 1, 2$, where $\boldsymbol{\epsilon}$ was drawn from a multivariate normal distribution with mean $\mathbf{0}$, $\mathrm{Var}[\epsilon_1] = \mathrm{Var}[\epsilon_2] = 1$, and $\mathrm{Cov}[\epsilon_1, \epsilon_2] = 0.5$. $\mu(\boldsymbol{X})$ was fixed to be $1 + \boldsymbol{X}_1 + 2\boldsymbol{X}_2 + 0.5\boldsymbol{X}_3 + \boldsymbol{X}_4$ for all simulation scenarios. Table 2.1 describes choices of $c(\boldsymbol{X})$ and $\delta_{A_1}(\boldsymbol{X})$ defining four scenarios.

Table 2.1: The interactive and carryover effects for the five simulation scenarios.

Scenario	$c(\boldsymbol{X})$	$\delta_{-1}(\boldsymbol{X})$	$\delta_1(\boldsymbol{X})$
1	$1.12(0.3 - X_1 - X_2)$	0	0
2	$1.15(X_1 - 1.25X_2^2)$	0	0
3	$1.12(0.3 - X_1 - X_2)$	$\left\lvert\frac{\mu(\boldsymbol{X})+c(\boldsymbol{X})}{4}\right\rvert$	$\left\lvert\frac{\mu(\boldsymbol{X})-c(\boldsymbol{X})}{2}\right\rvert$
4	$1.15(X_1 - 1.25X_2^2)$	$0.4X_1^2 + 0.3X_2$	$1 - 2X_1 - X_2^2$

Scenarios 1 and 3 are linear in $\boldsymbol{X}$, whereas Scenarios 2 and 4 are nonlinear. Note that scenario pairs $(1, 3)$ and $(2, 4)$ are similar, but Scenarios 3 and 4 include carryover effects. The optimal ITR was estimated via crossover GOWL using a Gaussian kernel. The penalty parameter, λ_n, and the Gaussian kernel bandwidth parameter, σ_n, were selected using 5-fold cross-validation on the grids $[0.1, 0.5, 1, 5, 10, 50, 100, 500]/n$ and $[0.1, 0.2, \ldots, 5.0]$, respectively. In scenarios where carryover effects are present, RLT (Zhu et al., 2015) was used to fit both models to estimate $\widehat{\delta}_{A_1}(\boldsymbol{X})$ using Algorithm 2.1.

A testing data set of size $n_{\text{test}} = 10,000$ was generated similarly with period 1 data only. The misclassification rate, or $\mathbb{P}_{n_{\text{test}}} 1\left\{\widehat{D}^*(\boldsymbol{X}) \neq D_0(\boldsymbol{X})\right\}$, of the estimated ITR applied to the

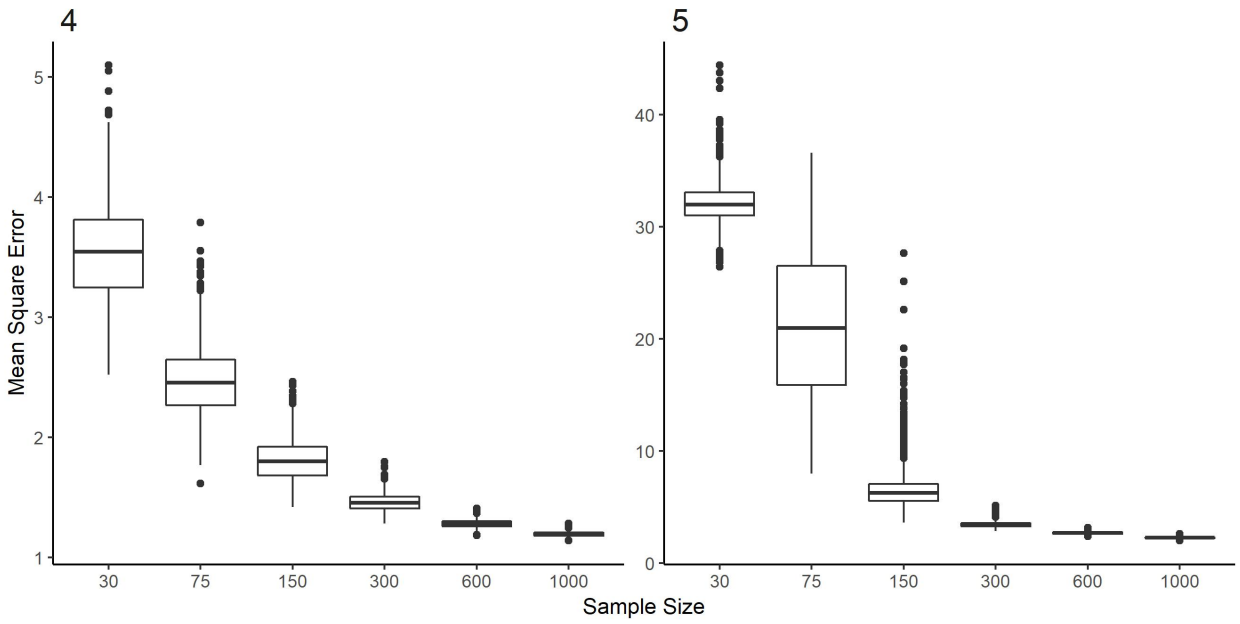

Figure 2.1: Boxplots of mean square error for RLT predicted $\delta_{A_1}(X)$ on the testing set compared with the true carryover.

testing set was calculated, where $\mathbb{P}_{n_{\text{test}}}$ is the empirical mean in the test set. We also calculated the estimated value of the estimated ITR, $\widehat{\mathcal{V}}\left(\widehat{D}^*\right)$ (Qian and Murphy, 2011), where

$$\widehat{\mathcal{V}}(D) = \frac{\mathbb{P}_{n_{\text{test}}}[Y1\{A = D(\boldsymbol{X})\}/P(A_1|\boldsymbol{X})]}{\mathbb{P}_{n_{\text{test}}}[1\{A = D(\boldsymbol{X}\}/P(A_1|\boldsymbol{X})]}. \tag{2.6}$$

Note that $P(A_1|\boldsymbol{X}) = 0.5$ is constant here. The estimated value is the average reward observed under the estimated optimal ITR when applied to the testing set. Figure 2.1 displays the mean square error from estimating the carryover effects with RLT for Scenarios 3 and 4.

Simulations were repeated 1,000 times at training set sample sizes of 30, 75, 150, 300, and 600. Comparisons to OWL, GOWL, and ridge regression methods in the parallel setting were made. For OWL and GOWL, a Gaussian kernel was used, and the aforementioned grids for λ_n and σ_n are considered in 5-fold cross-validation. For ridge regression, the model includes all covariates and treatment-covariate interactions without any higher order terms or between-covariate interactions. 5-fold cross-validation was used to determine a value for the the ridge penalty parameter, where the same values for λ_n in the OWL methods are considered. All simu-

lations were performed with R version 3.4.3 (R Core Team, 2017). RLT was implemented with the RLT package, version 3.2.1 (Zhu, 2017), and all OWL methods were implemented with the DynTxRegime package, version 3.2 (Holloway et al., 2018). While the DynTxRegime package does not currently support GOWL, the inputs for OWL can be recoded to implement GOWL. Ridge regression was carried out with the glmnet package (Friedman et al., 2010).

Figure 2.2 displays the average misclassification rates across all sample sizes, methods, and scenarios. Figure 2.3 displays the mean square error of the estimated value from the true value, i.e., $\mathbb{P}_{n_{\text{test}}}\left\{\left[\widehat{\mathcal{V}}\left(\widehat{D}^*\right)-\widehat{\mathcal{V}}\left(D_0\right)\right]^2\right\}$ from period 1 data. On average, crossover GOWL yields lower misclassification rates and higher estimated values at smaller sample sizes across all scenarios, despite the potential for a high mean square error when estimating $\delta_{A_1}(\boldsymbol{X})$. Crossover GOWL shows marked improvement in both misclassification and estimated value for small n. When n is large, ridge regression yields competitive results with that from crossover GOWL, but crossover GOWL still appears to have marginal gains. Although GOWL in the parallel setting does not perform as well as OWL in any of the presented scenarios, Chen et al. (2018) discuss scenarios where improvements in misclassification and estimated value are observed when using GOWL as opposed to OWL.

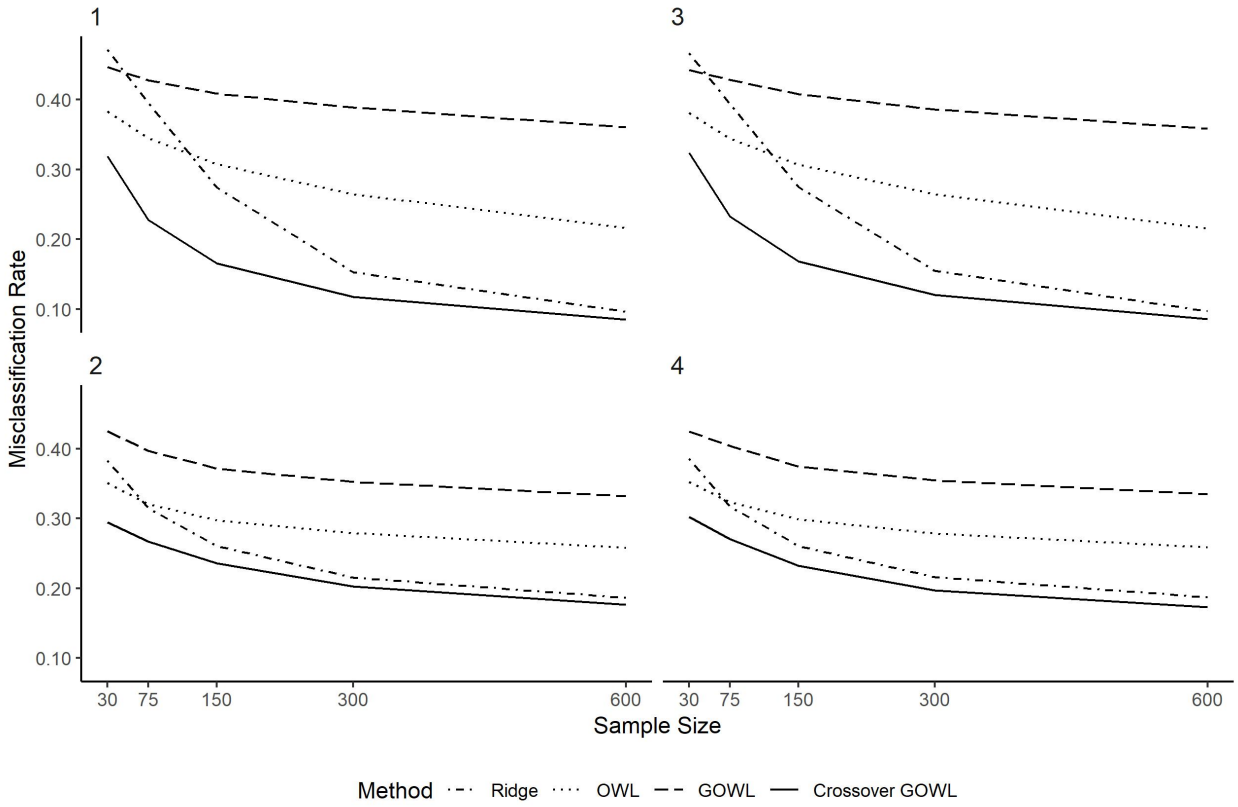

Figure 2.2: Mean misclassification rate of 1,000 simulations for estimating the optimal ITR, applied to a testing set of size 10,000 for each of 4 simulation scenarios.

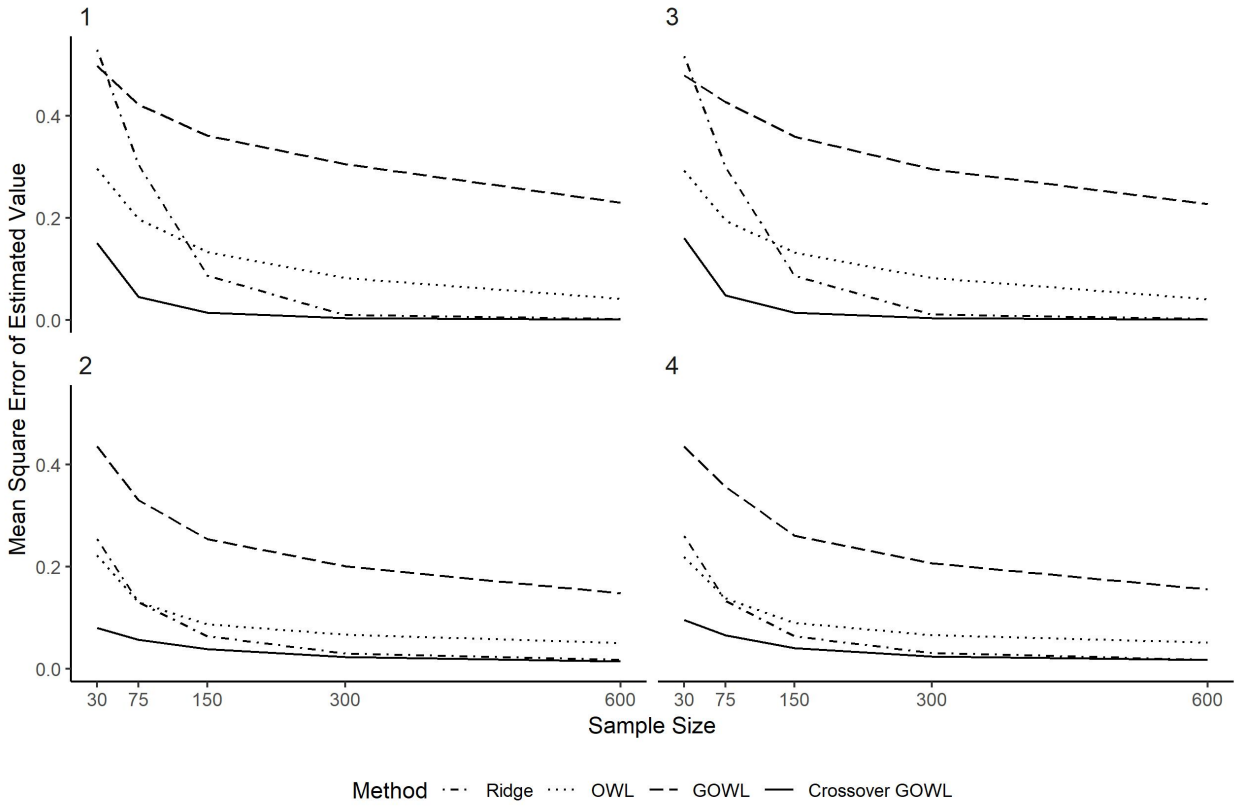

Figure 2.3: Mean square error of the estimated value compared to the true value from 1,000 simulations for estimating the optimal ITR, applied to a testing set of size 10,000 for each of 4 simulation scenarios.

2.5 Optimizing Satiety from the Food, Adolescents, Mood and Exercise Trial

We present the application of crossover GOWL to data from the Food, Adolescents, Mood and Exercise (FAME) crossover feeding trial, conducted at the University of Southern California (USC) (O'Reilly et al., 2015). The FAME trial included African American and Latino adolescents who were overweight or obese. African American and Latino adolescents are disproportionately affected by overweight and obesity outcomes compared to their non-Hispanic counterparts (Ogden et al., 2014; O'Reilly et al., 2015; Taveras et al., 2013). Dietary intake is a major modifiable risk factor and represents a key intervention point in improving weight loss (Bleich et al., 2017; Kipping et al., 2008). One promising approach is to modify dietary components to improve satiety to indirectly reduce caloric intake (Anderson et al., 2009). In epidemiologic studies of adults in the US, fiber intake is inversely associated with body weight and body fat (Slavin, 2005), even after adjusting for confounding factors such as dietary fat intake. However, results from intervention studies are mixed: increased dietary fiber intake has been shown to have varied effects on body weight among adults who are overweight or obese, with limited research in pediatric or adolescent populations (Rössner et al., 1987; Ryttig et al., 1989; Slavin, 2005; Thompson et al., 2005; Tucker and Thomas, 2009). Given the heterogeneity in the effects of dietary fiber intake on body weight, it is essential to identify the subgroups of overweight and obese adolescents who may benefit from tailored clinical advice to increase fiber intake. We estimate a decision rule to identify a subgroup of adolescents who are overweight or obese that experiences larger increases in patient-reported satiety from a high fiber diet as opposed to the more common high sugar diet.

This study was conducted at the USC Health Sciences campus in Los Angeles, California from 2008 to 2011. Eighty-six Latino and African American adolescents (ages 14 to 17 years of age) who were overweight or obese (body mass index (BMI) percentile $> 85\%$) were recruited. Race was self-reported, and subjects were included if all four grandparents were Latino or African American. Subjects were excluded if they had type 2 diabetes, were in a weight loss program within the past 6 months, or used medications that influenced insulin or body compo-

sition. Informed written parental consent and participant assent were acquired before all testing procedures. The Institutional Review Board of USC approved all study procedures.

Participants received either a high sugar/low fiber (HSLF) meal plan or a high fiber/low sugar (HFLS) meal plan for breakfast and lunch on two separate visit days. Participants were randomized with equal probability to receive the HSLF/HFLS or HFLS/HSLF sequence with a minimum 2 week washout period between visits. The meals were isocaloric and matched for macronutrients except sugar and fiber content. Participants initially attended a baseline visit at the Clinical Trials Unit at the USC University Hospital where insulin sensitivity, Tanner stage via examination by a medical professional, BMI percentile for age, sex, ethnicity, waist circumference, and hemoglobin A1c (HbA1c) were collected. Insulin sensitivity was assessed via a frequently sampled intravenous glucose tolerance test and calculated using the minimal model (Bergman et al., 1979; Yang et al., 1987). At the subsequent test meal visits, participants received either a HSLF or HFLS breakfast after a 10 hour overnight fast. At noon, the participants received the same meal condition for lunch. Participants rated their hunger and fullness via a 100 mm-visual analog scale (VAS) prior to breakfast and 45 minutes after the start of lunch (300 minutes after breakfast). Participants were provided with age appropriate activities between meals (e.g., video games, crafts, books, etc.).

The satiety outcomes are formally defined as the negative change in hunger, since lower values of hunger are desired, and the observed change in fullness between 8:00 AM and 1:00 PM (before breakfast and after lunch). Due to the nature of the outcomes, the required 10 hour overnight fast, and the implemented minimum 2 week washout period, we assumed no carryover effects were present. Of the 86 subjects who completed the study, 20 were removed for missing outcomes, and 1 was removed for missing insulin sensitivity. Participants that did not return within 5 weeks were also removed $(n = 54)$. We compared crossover GOWL with OWL, GOWL, and ridge regression using data from period 1 only. Methods were implemented as described in Section 2.4. 5-fold cross-validated value estimates were obtained, but rather than using Equation (2.6) which uses only period 1 data, the value for each observation $i = 1, \ldots, n_m$ in the mth

Table 2.2: Mean (sd) 5-fold cross-validated estimated values for feeding trial data compared with the observed value from period 1.

	Outcome			
	Fullness		Hunger	
Ridge	3.00	(4.53)	5.60	(8.15)
OWL	3.07	(3.88)	5.45	(7.42)
GOWL	3.85	(4.97)	8.29	(7.93)
Crossover GOWL	6.39	(3.57)	10.50	(8.36)
Observed	0.96		4.66	

fold's testing set was computed as $Y_{i,1}1\left\{A_1 = \widehat{D}_0(\boldsymbol{X})\right\} + Y_{i,2}1\left\{A_2 = \widehat{D}_0(\boldsymbol{X})\right\}$ where n_m is the size of the mth fold for $m = 1, \ldots, 5$. Although OWL, GOWL, and ridge regression were trained on period 1 data, data from both periods were used to improve accuracy in the value estimate because the testing set size for each fold is quite small.

Resulting estimated values, averaged across folds, are presented in Table 2.2 along with the mean outcome observed from period 1. For both outcomes, all methods show improvement in the estimated value in comparison to randomization, but crossover GOWL yields the highest improvement. For self-reported fullness, crossover GOWL also yields the smallest standard deviation. When training crossover GOWL on the full dataset, 92% (51%) of participants are assigned to the HFLS to maximize the change in fullness (hunger). A more detailed clinical interpretation of the estimated ITR along with the distribution of features across the groups assigned to HFLS and HSLF from crossover GOWL for both outcomes are presented in Appendix A. Dietary fiber is recommended to improve overall health in the general population (Marlett et al., 2002); however, the estimated ITRs from hunger and fullness may inform the development of tailored dietary intake advice for subgroups of at-risk adolescents.

2.6 Discussion

Precision medicine is an emerging field with rapid developments in analysis methods; however, these advancements typically revolve around parallel designs. This paper proposes the combined use of crossover designs and generalized outcome weighted learning for the purpose

of estimating optimal ITRs. The proposed method addresses a key gap in the literature; little to no work has been done to better involve crossover designs in precision medicine, despite how naturally crossover studies lend themselves to the field. Kulasekera and Siriwardhana (2018) propose a ranking method to estimate the optimal ITR from a crossover study but provide no recommendations on how to deal with carryover effects. In contrast, crossover GOWL is able to handle such effects. Furthermore, regardless of the presence of carryover effects, the proposed method shows improvements in the estimated value and misclassification rate, especially at the smaller sample sizes typical of crossover designs compared to standard methods with the parallel group design.

An alternative to GOWL that has been developed is residual weighted learning (RWL) (Zhou et al., 2017). RWL is an extension of OWL that weights the misclassification error by residuals from a model fit to the outcome instead of the observed rewards themselves. Unlike GOWL, RWL uses a non-convex loss function that does not guarantee global minimization (Tao, 2005). In the proposed method, there is no need to include residuals in the weight, because the residuals would cancel when taking the difference between responses to each treatment. Thus, the proposed method avoids specifying a model for the main effect of the covariates.

We note that when the distribution of $\widetilde{A_1} = \text{sign}\{R\} A_1$ is poorly allocated, the cross-validation mechanism for estimating λ_n and σ_n^2 may fail. If there is prior knowledge on the distribution of $\text{sign}\{R\}$, investigators could adjust randomization probabilities when assigning patients to treatment sequences accordingly. Otherwise, it is possible for a training set to not observe at least one $\widetilde{A}_1 = 1$ or $\widetilde{A}_1 = -1$. Lastly, there may be low power in testing $H_0 : E[\delta_{A_1}(\boldsymbol{X})] = 0$ at smaller sample sizes.

Several extensions of estimating the optimal ITR from crossover data are yet to be explored. For example, only the 2×2 design was studied in this paper. For larger design schemes, the proposed method could be implemented in a series of binary classifiers as in Dietterich and Bakiri (1994). Alternatively, one could expand crossover GOWL to multi-category classification. There have been several developments in multi-category support vector machines (Lee et al., 2004;

Zhu et al., 2004). More recently, Liang et al. (2018) propose an outcome weighted deep learning method to estimate the optimal ITR for multiple treatments. Another possible extension is to consider the residual from modeling the treatment response difference as the observed reward. Fu et al. (2016) and Zhou et al. (2017) have seen favorable results using residual weights, but further improvements may come from using the residuals in outcome weighted learning with the piece-wise hinge loss from GOWL. Finally, the proposed method could be improved upon with methods for variable selection. For example, the L_1 penalty could be imposed during optimization to simultaneously restrict model complexity and perform variable selection as suggested by Chen et al. (2018), Song et al. (2015), Xu et al. (2015), and Zhou et al. (2017).

CHAPTER 3: FEATURE-GUIDED CLUSTERING

3.1 Introduction

We now discuss a different objective of precision medicine: identifying a subset of homogenous disease subgroups within a heterogeneous population using clinical presentation rather than treatment-response. These subgroups may be conceptualized as disease phenotypes, or cohorts of patients who share a disease diagnosis but are distinct with regards to their genomic, biochemical, or clinical data (Haendel et al., 2018). For example, there is general aggrement in the medical community that there exist somewhere from 2-9 phenotypes of asthma that may be defined by biomarkers and/or patient history (Kosorok and Moodie, 2015; Lötvall et al., 2011; Lowe et al., 2005; Wenzel, 2006). Characterizing the different asthma phenotypes aids in specifying aspects of the asthma pathophysiology that are most relevant to a given patient and allow for more precise prediction of disease prognosis or assignment to therapeutic regimes. The definition of disease phenotypes is specific and relies heavily on domain knowledge to define phenotypic subgroups that are meaningfully different whilst sufficiently homogenous, such that differentiated recommendation or therapies may be provided to each stratus that is effective, cost-effective, and minimizes the prevention of harm (Burton et al., 2012; Haendel et al., 2018). In this chapter, we propose a novel clustering method that leverages the information in patient-specific factors that may correlate with the phenotypes of interest to guide the clustering method. This approach is particularly useful in settings where the disease phenotypes are expressed with great patient heterogeneity.

For example, type 1 diabetes (TID) is an autoimmune disease in which patients no longer produce insulin and are tasked with daily insulin administration and self-management of blood

glucose levels (American Diabetes Association, 2014; Hood et al., 2009). Diabetes management is particularly challenging in youth and adolescence (Miller et al., 2015). An unintended side-effect of insulin therapy is weight gain, and recent data shows that the prevalence of overweight and obesity is increasing in this population (Liu et al., 2010; DuBose et al., 2015). As a result, T1D patients present with a wide range of weight status and glycemic control, as measured by body mass index z-score (BMIz) and hemoglobin A1c (HbA1c), respectively. This profound heterogeneity in clinical presentation complicates the use of standard approaches to co-optimize weight and glycemic control across the population. Therefore, the identification and characterization of subgroups of youth with T1D who have a similar weight status and level of blood glucose control as distinct 'weight-glycemia phenotypes' of T1D could enable better outcomes across the population, as these subgroups would likely benefit from distinct therapeutic strategies and can be targeted more efficiently as groups for clinical recommendations. Although there exist clinical cut-points for BMIz and HbA1c (Petitti et al., 2009; Wang and Chen, 2012), these cut-points have not been validated in conjunction to jointly characterize subgroups based on weight status and glycemic control. Moreover, an exploratory approach is better suited for identifying real-life phenotypes to emerge rather than forcing a fit based on a-priori clinical cut-points for weight and glycemic control.

Some investigators approach subgroup identification as a clustering problem (Deliu et al., 2016; Jang et al., 2013; Park et al., 2015), by forming groups of observations such that members within the same group are more similar than members across different groups (Friedman et al., 2001; Hartigan and Wong, 1979; Ward Jr, 1963). There are only a few existing methods for a subclass of clustering, known as semi-supervised clustering, where clusters are associated with some outcome of interest. With semi-supervised clustering, the outcome is believed to be a noisy label or surrogate variable for the true underlying class (Bair, 2013). Bair and Tibshirani (2004) and Koestler et al. (2013) propose methods that perform variable selection among a set of features believed to be correlated with the outcome prior to clustering, and variables found to be most associated with the outcome are selected for cluster analysis while the remaining variables

are discarded. Gaynor and Bair (2017) combine this idea with sparse clustering (Witten and Tibshirani, 2010) by proposing preweighted sparse clustering to down-weight the "less significant" variables from variable selection rather than discarding them entirely. Preweighted sparse clustering thus induces sparsity in the set of clustered features while maximizing the between-cluster sum of squares. However, when the outcome is particularly noisy, conventional clustering and semi-supervised clustering methods may not accurately identify the true underlying disease subgroups (Gaynor and Bair, 2017). Moreover, the existing methods do not cluster directly on the phenotypic outcomes of interest, nor do they account for multivariate outcomes, which is often the case in clinical settings where positive outcomes and adverse events must be co-optimized. We therefore propose a new class of semi-supervised clustering in which a set of feature variables may be used to denoise, or smooth, the surrogate outcomes; clustering algorithms are then applied to a weighted average of the observed and denoised outcomes.

3.2 Methodology

Assume we observe i.i.d. data $(\boldsymbol{X}_i, \boldsymbol{Y}_i)$, for $i = 1, \ldots, n$, where $\boldsymbol{X} \in \mathcal{X} \subset \mathbb{R}^p$ is a matrix of feature or predictor variables, and $\boldsymbol{Y} \in \mathcal{Y} \subset \mathbb{R}^q$ is a matrix of continuous outcomes believed to define the disease phenotypes.

We propose calculating a weighted average of the observed and fitted outcomes, or

$$\widetilde{\boldsymbol{Y}} = \boldsymbol{Y}\boldsymbol{W} + \widehat{\boldsymbol{Y}}(\boldsymbol{I}_q - \boldsymbol{W}), \text{ subject to } 0 \leq w_m \leq 1,$$

for $m = 1, \ldots, q$. Here, $\widehat{\boldsymbol{Y}}$ are the predicted values of $\boldsymbol{Y}$, obtained from regressing each Y_m on $\boldsymbol{X}$. Any regression technique for which consistency holds may be used. In this chapter, we will use random forests (Breiman, 2001) for all displays of implementation. $\boldsymbol{I}_q$ is the $q \times q$ identity matrix, and $\boldsymbol{W} = \text{diag}(w_1, \ldots, w_q)$ is a diagonal matrix of weights, allowing each variable to be assigned a distinct weight in the case that some outcomes are noisier than others. Cluster methods may then be applied to $\widetilde{\boldsymbol{Y}}$, such as k-means (Hartigan and Wong, 1979) or hierarchical

clustering (Ward Jr, 1963). Using $\widetilde{\boldsymbol{Y}}$ informs the clustering algorithm not only by the smoothed outcomes, $\widehat{\boldsymbol{Y}}$, but also by the residual information in $\boldsymbol{Y}$.

To specify $\boldsymbol{W}$, we recommend maximizing the average silhouette width (Rousseeuw, 1987), an internal validation of a given clustering that represents a non-linear combination of within-cluster connectivity and between-cluster separation (Brock et al., 2011), in a grid search. However, the user may choose any method of cluster validation, e.g., the Dunn Index (Dunn, 1974), connectivity (Handl et al., 2005), or average proportion of non-overlap (Yeung et al., 2001). We also recommend standardizing $\boldsymbol{Y}$ and $\widehat{\boldsymbol{Y}}$ prior to clustering to prevent outcomes with higher means and variances to be considered equally in the clustering process.

Note that $\boldsymbol{Y}$ need not be continuous. A logistic regression may be used for binary or ordered outcomes, and classification methods may be used for unordered categorical outcomes. Relevant cluster methods may then be applied for mixed outcomes, such as those proposed by Ahmad and Dey (2007), Chiu et al. (2001), or Hsu and Huang (2008). The choice of k is beyond the scope of this chapter.

3.3 Numerical Experiments

To demonstrate the performance of the proposed method, we performed simulations varying the sample size, n, and the number of feature variables correlated with the true clustering, p_e. The true classification contained three classes, with 25% of the observations in each of the first two classes, and the remaining 50% in the third class. Three outcomes were generated from normal distributions with means $(1, 1, -1)$, $(0, 1, -1)$, and $(0, 0, 0)$ for each class, respectively, and a standard deviation of 1 (Figure 3.1). The features were generated as follows

$$X_{ij} = \begin{cases} 1 + \epsilon_{ij}, & \text{if } i \leq n_1, j \leq p_e \\ -1 + \epsilon_{ij}, & \text{if } i > (n_1 + n_2), j \leq p_e \\ \epsilon_{ij}, & \text{otherwise,} \end{cases}$$

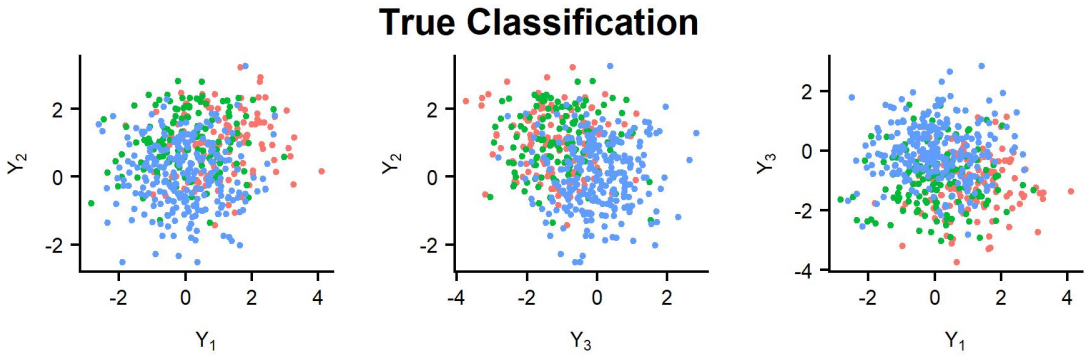

Figure 3.1: Scatter plots showing the bivariate distributions of a simulated $\boldsymbol{Y}$, colored by the true underlying class labels.

where n_h is the size of class $h = 1, 2, 3$, $p_e < p = 50$, and $\epsilon_{ij} \sim N(0, 1)$.

$\widehat{\boldsymbol{Y}}$ was estimated via random forest (Breiman, 2001), and both $\boldsymbol{Y}$ and $\widehat{\boldsymbol{Y}}$ were standardized. Average silhouette width was calculated across the grid $[0.0, 0.1, \ldots, 1.0]$ for each w_m, $m = 1, 2, 3$ to determine the optimal choice of weights. The proposed method was applied in conjuction with both k-means and hierarchical clustering, and comparisons were made to traditional k-means and hierarchical clustering alone. For both proposed and traditional hierarchical clustering, complete linkage and Euclidean distance were used to determine cluster assignments. Resulting clusters were evaluated by the adjusted Rand index (ARI) (Hubert and Arabie, 1985), a measure for how well cluster assignments match with the truth; values closer to 1 are desired. For all analyses, k was fixed to be correctly chosen as 3, but n and p_e were varied across $[50, 100, 250, 500, 1000, 1500, 2000]$ and $[5, 10, 15, 20]$, respectively.

Examples of a solution under each method with $n = 500$ and $p_e = 25$ are displayed in Figures 3.2-3.5. Visually, the conventional methods are unable to capture the degree of overlap that is true to the data generation. In contrast, the proposed methods allow the cluster assignments to be "friendlier" and more generous with the potential overlap.

Each simulation was replicated 1,000 times, and the mean ARI is displayed in Figure 3.6. On average, the proposed method performs much better than traditional methods alone. In the best case scenario, with a large sample size and large p_e, the proposed method on average yields an ARI that is 0.769 points higher than traditional methods. k-means tends to perform slightly better

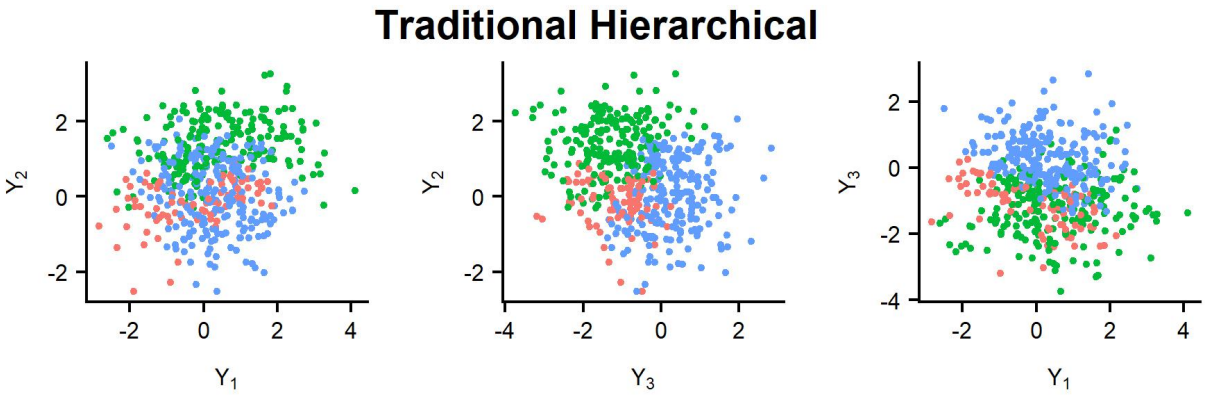

Figure 3.2: Example cluster assignments from a single simulation using traditional hierarchical clustering.

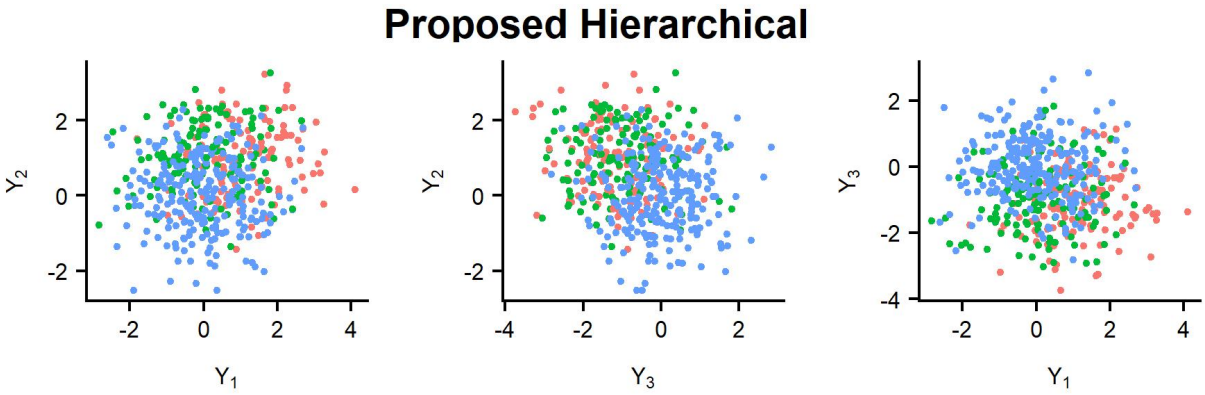

Figure 3.3: Example cluster assignments from a single simulation using the proposed method with hierarchical clustering.

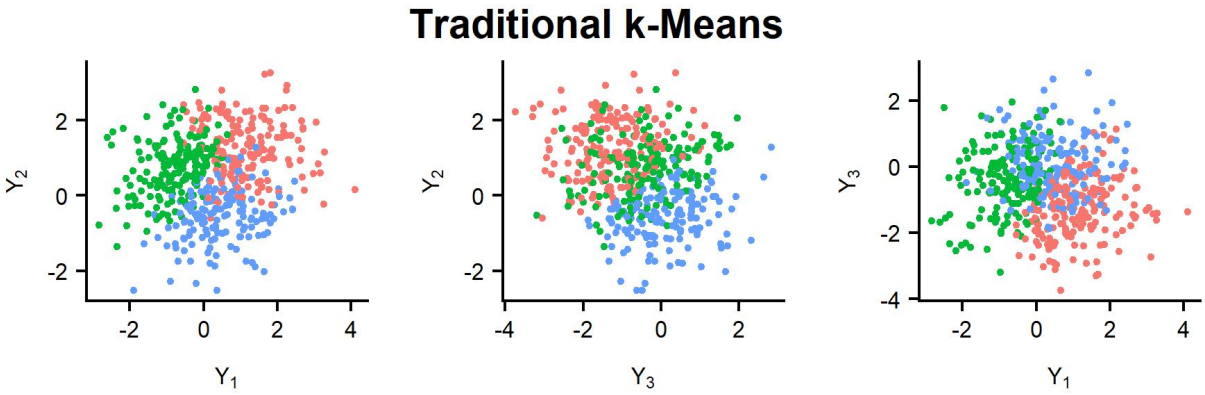

Figure 3.4: Example cluster assignments from a single simulation using traditional k-means clustering.

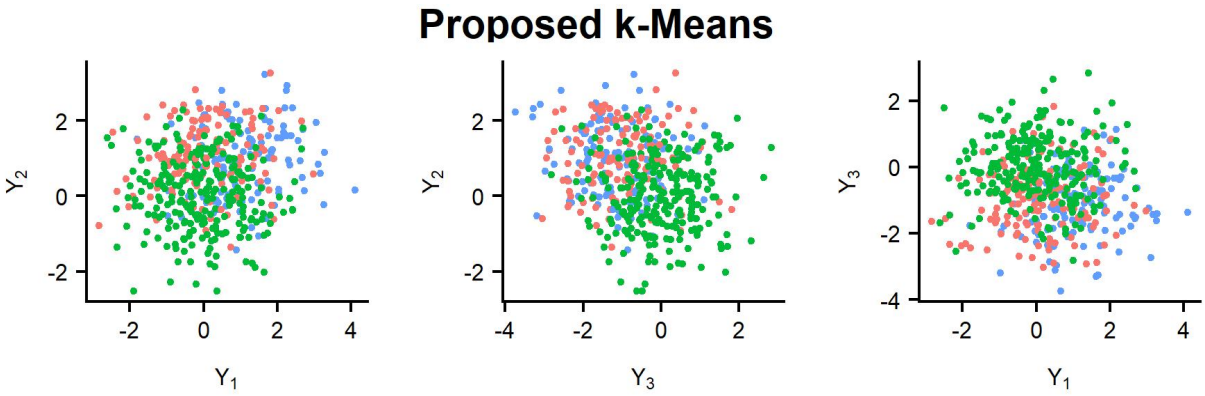

Figure 3.5: Example cluster assignments from a single simulation using the proposed method with k-means clustering.

on average than hierarchical clustering, except for the proposed method when $p_e = 5$ where the two methods are more or less equivalent. Figure 3.7 depicts the mean of the optimized weights in the proposed method for both hierarchical and k-means clustering. Overall, the two methods agree on weights, signifying stability in the choice of weights, and there is a monotone decreasing trend as n and p_e increase. Thus, there is less and less reliance on the observed outcomes $\boldsymbol{Y}$, and more on the fitted outcomes $\widehat{\boldsymbol{Y}}$ as the signal in $\boldsymbol{X}$ increases.

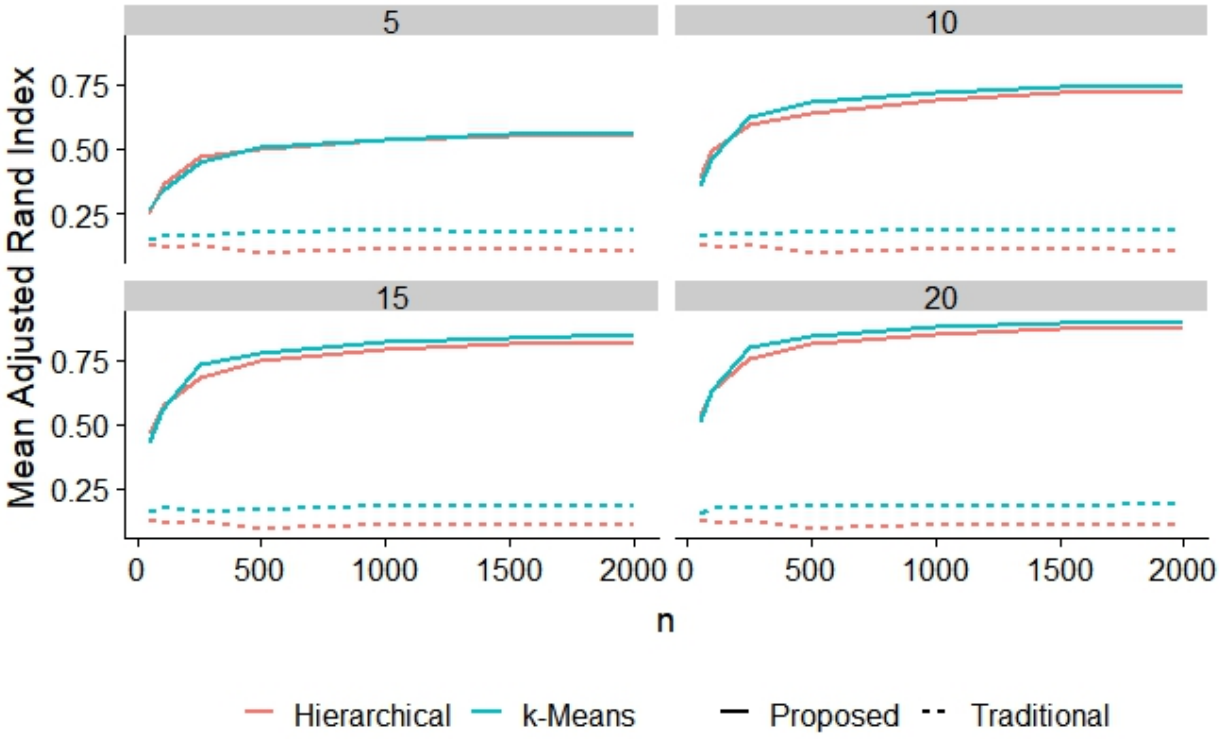

Figure 3.6: Mean ARI across 1,000 replications, comparing the proposed method to traditional methods at varying sample sizes and values of p_e.

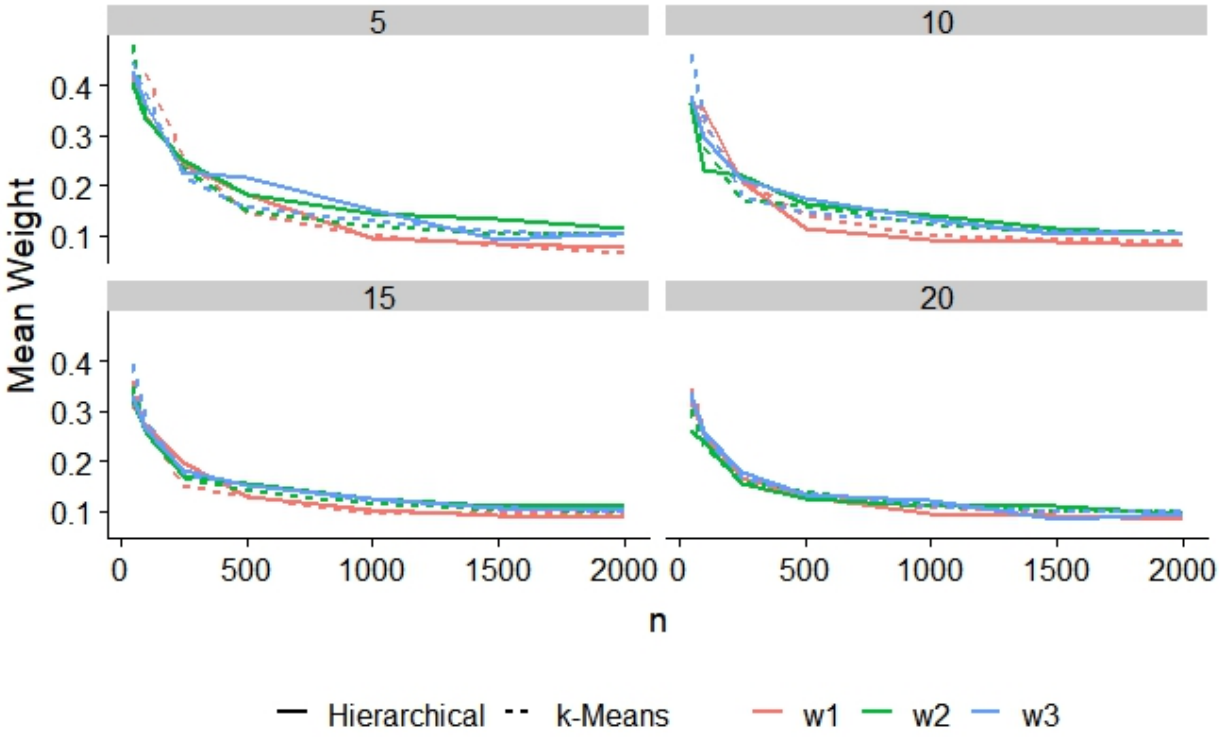

Figure 3.7: Mean of chosen weights across 1,000 replications, comparing hierarchical and k-means clustering weights at varying sample sizes and values of p_e.

3.4 Weight-Glycemia Subtypes of Type 1 Diabetes

Since the widespread adoption of intensified insulin therapy for the prevention of diabetes complications (e.g., heart disease, neuropathy, retinopathy, and nephropathy) in 1993 (Orchard et al., 2015), the clinical care of T1D has centered around achieving tight glycemic control. However, recent evidence show that many patients with T1D do not meet clinical targets for HbA1c levels, particularly among youth and young adults (Foster et al., 2019). Additionally, the technologies meant to keep blood glucose normal may promote weight gain in some individuals (Purnell et al., 2017, 1998). The increasing prevalence of obesity in T1D has been attributed to decreased glucosuria with tighter glucose control, increased caloric intake to treat hypoglycemia, increased lipogenesis and fat accumulation, and decreased catabolism associated with peripheral hyperinsulinemia, which are needed to suppress hepatic glucose production (Corbin et al., 2018; Driscoll et al., 2017). Since the obesity- and glycemia- associated risk factors for cardiovascular disease and other diabetic complications begin to accumulate early in life, it is imperative for clinical strategies to promote and support youth and young adults with T1D in maintaining tight glycemic control as well as a healthy weight.

The evolution of T1D to include overweight and obesity, combined with the complicated physiologic relationships between weight and glycemia, pose a challenge to understand the population-level associations between BMIz and HbA1c in a way that informs meaningful strategies to co-optimize both outcomes. For example, it is not well understood how overweight and obesity distribute across levels of glycemic control, and whether weight status can be used to universally infer information about glycemic control, or vice versa, and how these outcomes interact to form more nuanced clinical phenotypes of T1D. Weight-glycemia phenotypes may confer information about goals for treatment and effectiveness of specific therapeutic strategies for optimizing outcomes simultaneously, especially given that weight gain may be an unintended consequence of intensive insulin therapy in some individuals (Purnell et al., 2017).

We therefore aim to identify weight-glycemia subtypes of T1D using data from the SEARCH for Diabetes in Youth Study, a large nationally-representative observational cohort study of childhood diabetes in the US (Hamman et al., 2014; Liu et al., 2010). A subset of participants with newly diagnosed diabetes who attended both baseline and cohort visits, had a diagnosis of diabetes for at least 5 years, and were at least 10 years of age were included in the analysis. The proposed method was guided by a select set of features including sociodemographic characteristics (age, gender, race, maximum parental education, etc.), clinical characteristics (insulin dose, insulin regimen, history of severe hypoglycemia or diabetic ketoacidosis, etc.), and psychosocial or behavioral characteristics (e.g., quality of life and smoking status).

Data from the cohort 1 visit were used. Figure 3.8 displays the distribution of BMIz and HbA1c for all included study participants. Multiple densities are not apparent from this figure, so traditional clustering techniques are likely to fail at accurately classifying patients together in T1D weight-glycemia phenotypes. Four subjects were excluded for having inconsistent answers to certain questionnaire items, e.g., responding "No" to having any hypoglycemic events in the past 6 months but also reporting values greater than 0 for the number of hypoglycemic events in the last 6 months. 183 subjects were removed for missing at least one of the outcome variables (BMIz and HbA1c), yielding a sample size of $n = 1,817$ for analysis. At most, 15% of any one feature variable was missing, and the missForest algorithm was implemented to impute those missing values (Stekhoven and Bühlmann, 2012; Stekhoven, 2013).

We partitioned the data into a training and testing set, 70% and 30%, respectively. We then applied the proposed method to the training set in R, version 3.4.1 (R Core Team, 2017), using the randomForest (Liaw and Wiener, 2002) to obtain $\widehat{\boldsymbol{Y}}$ and the cluster package (Maechler et al., 2017) to calculate average silhouette width when choosing $\boldsymbol{W}$ and k. The grids for selecting k and each w_m were $[4, \ldots, 9]$ and $[0.0, 0.1, \ldots, 1.0]$, respectively. $\boldsymbol{Y}$ and $\widehat{\boldsymbol{Y}}$ were standardized prior to optimization. Data were clustered using hierarchical clustering with complete linkage and Euclidean distance in both the proposed and traditional methods. For hierarchical cluster-

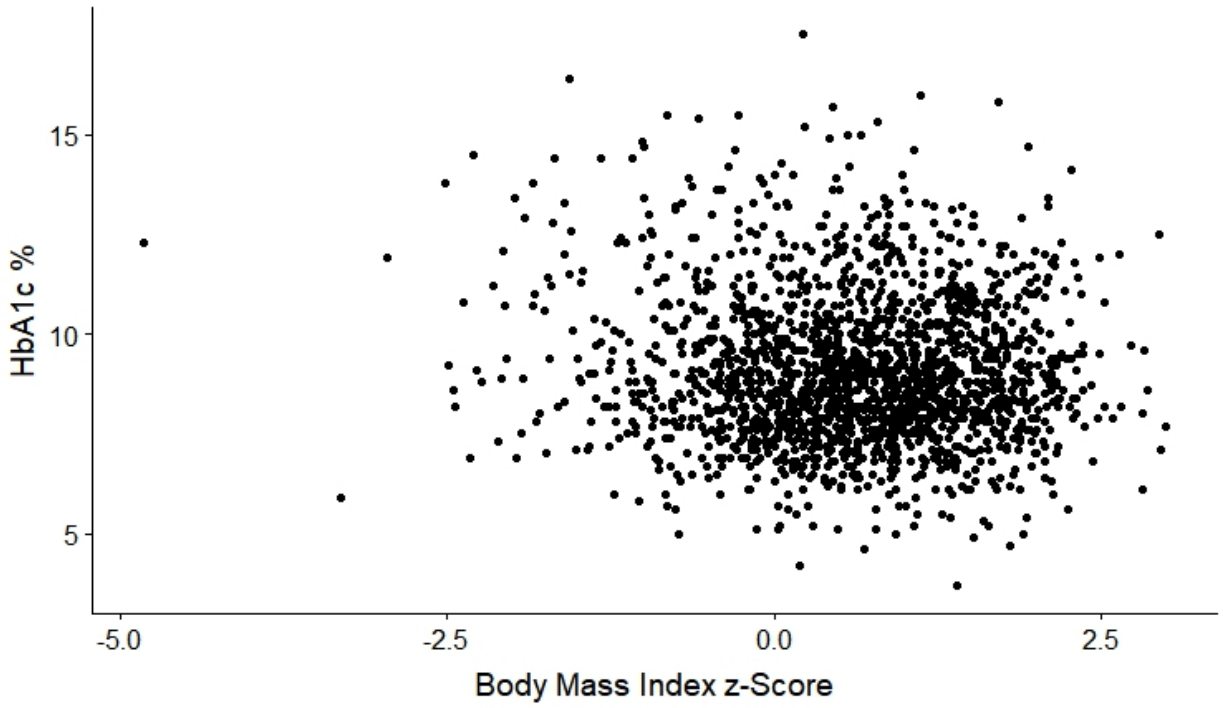

Figure 3.8: Scatter plot of weight and glycemia outcomes for type 1 diabetic adolescents.

ing, the number of clusters, k, was chosen by average silhouette width in the NbClust package (Charrad et al., 2014a).

To assess the clusters, a random forest classifier was fit for both methods, and cluster assignments were predicted in the test dataset for evaluation. Clustering by the traditional approach produced four clusters, but the sample size of the fourth cluster in the training data was very small ($n_4 = 2$). None of the testing data were assigned to the fourth cluster. The traditional method also produced very "clean" clusters (Figure 3.9); although the outcomes are very noisy, hierarchical clustering achieves clear separation in the estimated clusters. While visually attractive, this finding is concerning given the inability of the algorithm to separate meaningful variability (i.e., clinical heterogeneity) from measurement error. Meanwhile, the proposed method yielded a total of six clusters with a larger amount of visual overlap in BMIz and HbA1c (Figure 3.10). The weights chosen were 0.2 for HbA1c and 0.3 for BMIz, further suggesting that there is great patient heterogeneity in the two measures such that a greater weight on the fitted values is necessary. The means for BMIz and HbA1c for both methods are presented in Table 3.1. The pro-

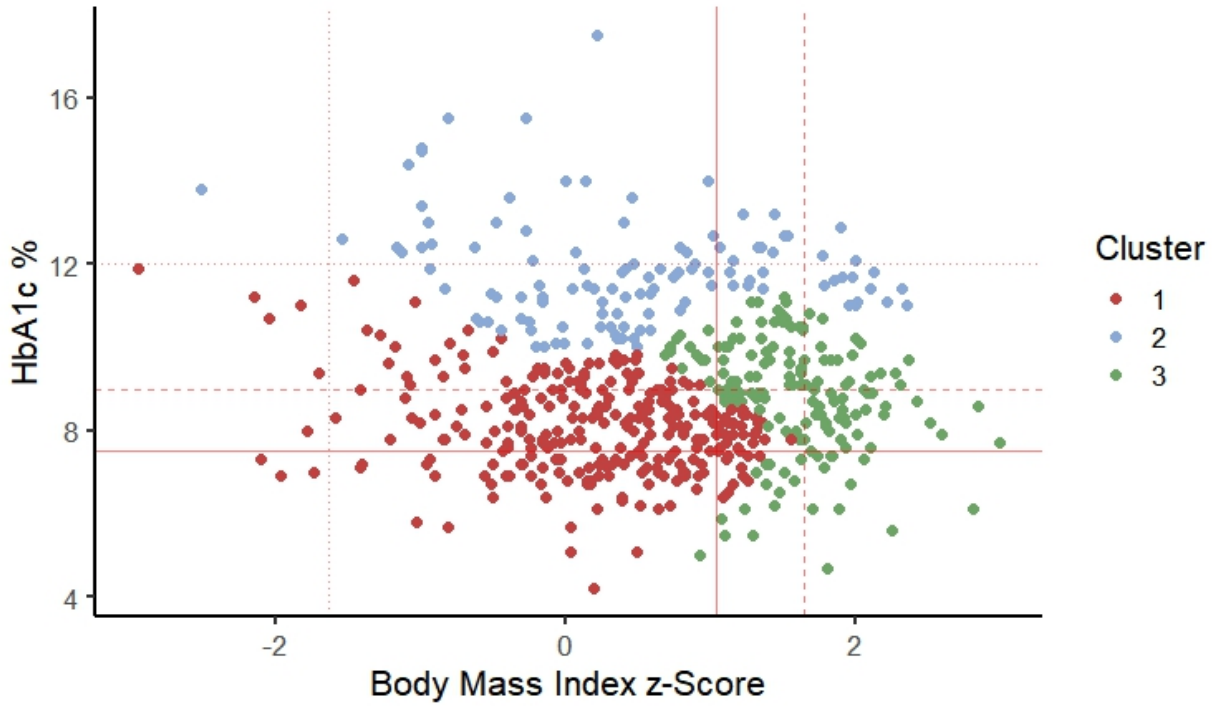

Figure 3.9: Scatter plot of weight-glycemia phenotypes in test dataset individuals, identified by traditional hierarchical clustering. Vertical lines denote cut-offs in age and sex adjusted BMIz for underweight, normal weight, overweight, and obese (Petitti et al., 2009). Horizontal lines denote cut-offs in HbA1c for normal, moderate, poor, and very poor glycemic control (Wang and Chen, 2012).

posed method outperforms traditional hierarchical clustering in its ability to find more granular subgroups with clinically distinct weight-glycemia phenotypes of T1D. Although the outcomes under the traditional method appear to be distinct across the three groups, a fourth group was negligible, and the remaining subgroups identified are no more clinically informative than a priori cut-offs used independently. However, outcomes under the proposed method suggest there are a variety of weight-glycemia combinations that comprise the T1D make up in adolescents.

Descriptive statistics on each cluster from the proposed method are reported in Table 3.2. Cluster weight status was classified as underweight, normal weight, overweight, or obese using cut-offs for mean BMIz of $-1.64, 1.04$, and 1.64, respectively (Wang and Chen, 2012). Cluster glycemic control was defined as good, moderate, poor, or very poor using cut-offs for mean HbA1c of $58, 75$, and 108, respectively (Petitti et al., 2009). Cluster 2 is typified by underweight

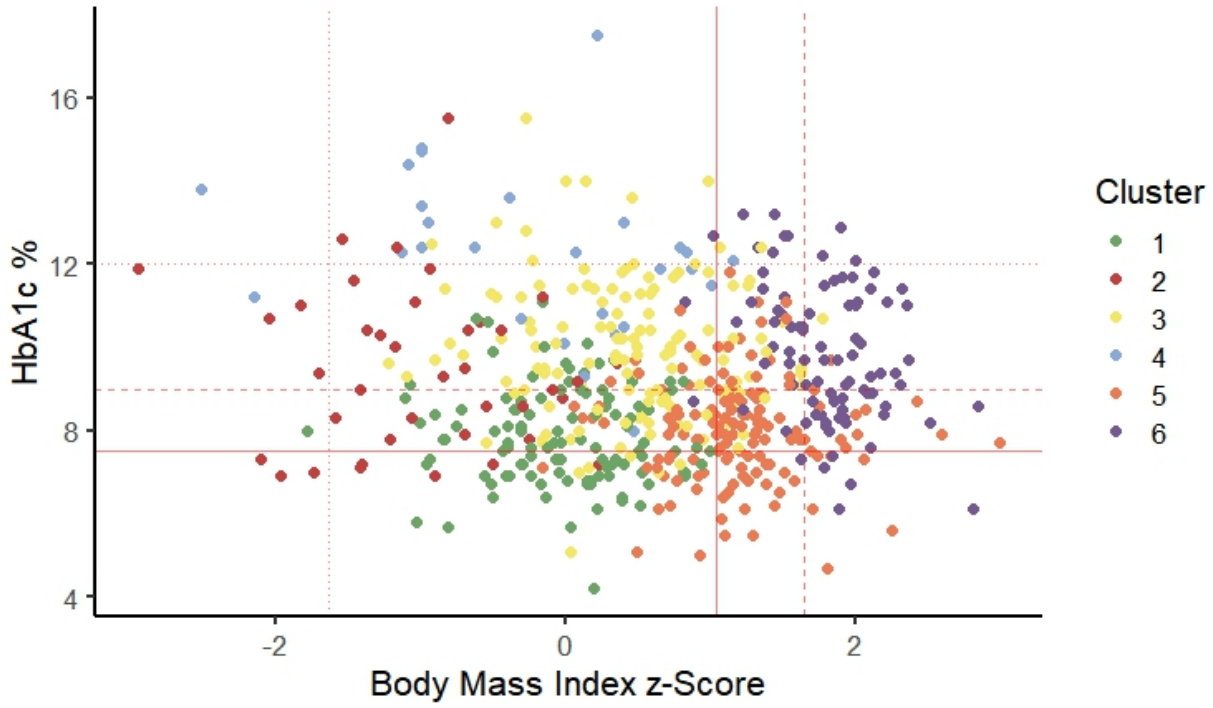

Figure 3.10: Scatter plot of weight-glycemia phenotypes in test dataset individuals, identified by the proposed clustering method. Vertical lines denote cut-offs in age and sex adjusted BMIz for underweight, normal weight, overweight, and obese (Petitti et al., 2009). Horizontal lines denote cut-offs in HbA1c for normal, moderate, poor, and very poor glycemic control (Wang and Chen, 2012).

Table 3.1: Mean (sd) body mass index z-score (BMIz) and hemoglobin A1c (HbA1c, %) for weight-glycemia phenotypes in the testing dataset, derived using traditional and proposed hierarchical clustering methods. Four clusters were identified in the training dataset using the traditional hierarchical clustering method, but none of the testing data were assigned to the fourth cluster.

Cluster	Traditional Method		Proposed Method	
	BMIz	HbA1c	BMIz	HbA1c
1	0.16 (0.80)	8.11 (1.14)	-0.04 (0.53)	7.88 (1.18)
2	0.43 (0.95)	11.82 (1.30)	-1.01 (0.72)	9.48 (1.45)
3	1.57 (0.44)	8.80 (1.35)	0.43 (0.61)	9.91 (1.66)
4	–	–	-0.21 (0.95)	12.24 (1.92)
5	–	–	1.18 (0.48)	0.85 (1.26)
6	–	–	1.79 (0.37)	9.83 (1.67)

and high HbA1c, suggestive of hypo-insulinemia and energy wasting through excessive glucosuria associated with sustained hyperglycemia, while Cluster 6 shows similarly elevated HbA1c that presents concurrently with elevated mean BMIz classified as obesity, which may be reflective of insulin resistance and poor metabolic health. Together, the clusters show that overweight and obesity present with varying degrees of glycemic control in the T1D patient population, implicating different therapeutic and clinical strategies to concurrently address weight and glycemia across subgroups.

Table 3.2: Selected feature variables according to weight-glycemia clusters in the SEARCH for Diabetes in Youth Study testing data. Table values represent means (sd) or counts (proportions) within each cluster.

	Total	Cluster 1	Cluster 2	Cluster 3	Cluster 4	Cluster 5	Cluster 6
n	546 (1.00)	39 (0.07)	27 (0.05)	109 (0.20)	140 (0.26)	140 (0.26)	89 (0.16)
BMIz	0.61 (0.97)	-0.04 (0.53)	-1.01 (0.72)	0.43 (0.62)	-0.21 (0.95)	1.18 (0.48)	1.79 (0.37)
HbA1c	9.09 (1.90)	7.88 (1.18)	9.48 (1.95)	9.91 (1.66)	12.20 (1.92)	8.05 (1.26)	9.83 (1.67)
Female	287 (0.53)	46 (0.42)	14 (0.36)	85 (0.61)	12 (0.44)	70 (0.49)	60 (0.67)
Age at Cohort Visit (years)	17.68 (4.34)	16.94 (5.09)	17.31 (4.47)	17.85 (4.05)	17.25 (3.29)	18.24 (4.64)	17.70 (3.39)
Age at Diagnosis (years)	9.89 (4.00)	9.31 (4.62)	10.09 (4.17)	9.83 (3.61)	9.25 (2.82)	10.41 (4.31)	9.99 (3.41)
Diabetes Duration (years)	7.74 (1.90)	7.59 (1.92)	7.18 (1.87)	7.97 (1.90)	7.95 (2.00)	7.79 (1.94)	7.67 (1.75)
Non-Hispanic White Race/Ethnicity	424 (0.78)	105 (0.96)	28 (0.72)	92 (0.66)	20 (0.74)	127 (0.89)	52 (0.58)
Parental Bachelor's degree or more	286 (0.53)	83 (0.76)	19 (0.49)	52 (0.37)	7 (0.26)	95 (0.67)	30 (0.34)
Private Health Insurance	398 (0.73)	101 (0.93)	26 (0.67)	94 (0.67)	8 (0.30)	122 (0.86)	47 (0.53)
Insulin Pump	306 (0.56)	84 (0.77)	25 (0.64)	54 (0.39)	7 (0.26)	97 (0.68)	39 (0.44)
Blood Glucose Monitoring $> 4\times$per day	376 (0.69)	98 (0.90)	26 (0.67)	70 (0.50)	13 (0.48)	113 (0.80)	56 (0.63)
Physical Activity	302 (0.55)	71 (0.65)	17 (0.44)	67 (0.48)	10 (0.37)	96 (0.68)	41 (0.46)
Physical Inactivity	277 (0.51)	37 (0.34)	20 (0.51)	84 (0.60)	20 (0.74)	65 (0.46)	51 (0.57)

Examination of clusters in relation to clinical cut-points for BMIz and HbA1c suggest that single outcome cut-points may be used to distinguish between certain subgroups (i.e., overweight and obese subgroups versus normal weight subgroups), but subgroups were not well delineated by both cut-points simultaneously. In fact, operation of cut-points for both weight status and glycemic control may split the identified weight-glycemia clusters and may not be as well-suited to identify subgroups sharing clinically significant, yet more nuanced, weight-glycemia phenotypes.

The weight-glycemia clusters identified show clinically significant differences in other individual characteristics according to phenotypic subgroups. For example, there were significant differences in the racial and ethnic breakdown across clusters (Table 3.2). Clusters 3-6 had the poorest glycemic control and were comprised of a higher proportion of non-Hispanic black youth (18.6%, 22.2%, and 21.4%, respectively, compared with 0.9% in Cluster 1). Meanwhile, Cluster 6, marked as the obese cluster, is comprised of the highest proportion of Hispanic youth (16.7% compared to 2.8% in Cluster 1). These patterns are consistent with previous studies showing that African-American, American Indian, Hispanic, and Asian/Pacific Islander youth with T1D are more likely to have higher HbA1c levels compared with non-Hispanic white youth (Kahkoska et al., 2018; Petitti et al., 2009) and the highest prevalence of overweight and obesity in the setting of T1D has been reported among those of Hispanic/Latino descent at approximately 46.1% (Minges et al., 2017). Cluster 1, which showed the most clinically favorable weight-glycemia phenotype (i.e. mean BMIz and HbA1c levels closest to clinical targets), also showed the highest markers of socioeconomic position, including maximum parental education and use of private health insurance. Subgroups with overweight and obesity comprised a higher proportion of females, consistent with multiple studies showing that females with T1D are more likely to be overweight and/or obese than males (Fröhlich-Reiterer et al., 2014; Manyanga et al., 2016; Minges et al., 2016, 2017). Additionally, these subgroups exhibit higher insulin pump use, which has been reported previously in the literature (Boucher-Berry et al., 2016; Fröhlich-Reiterer et al., 2014) but with mixed evidence (Garg et al., 2017; Mehta et al., 2017; Pańkowska et al., 2008).

Together, these findings confirm the heterogeneity in clinical presentation as well as underlying factors that may drive that presentation of disease, and the identified differences between subgroups may serve as key intervention points in future work to target treatment to the different needs across subgroups in precision medicine interventions.

3.5 Discussion

Cluster analysis remains a common choice in the identification of disease subgroups. However, to our knowledge, there are no proposed methods that cluster directly on the outcomes of interest with guidance from other patient factors. The proposed method takes this direct approach and, in contrast to semi-supervised clustering methods (Bair and Tibshirani, 2004; Gaynor and Bair, 2017; Koestler et al., 2013), accepts multivariate outcomes. The clinical significance of the proposed method lies in the use of multivariate outcomes as well as the applicability in scenarios where the outcomes are suspected to be extremely noisy surrogates for a true underlying class. Especially in the precision medicine setting, the proposed method shows promise in identifying clinically relevant disease subtypes, as we have shown in both simulation and analysis of the SEARCH for Diabetes in Youth dataset.

It is worth noting that such clinical applications require a great deal of guidance from a subject-matter expert. The outcomes $\boldsymbol{Y}$ must be carefully selected using subject-matter knowledge in contrast to traditional methods where several variables are clustered upon even though only a small subset of them may be important (Gaynor and Bair, 2017; Witten and Tibshirani, 2010). Additionally, to retain clinical interpretation of the resulting cluster assignments, it is not recommended to include high dimensional $\boldsymbol{Y}$.

There exist many avenues for future research with the proposed method. For example, selection of the number of clusters k remains a difficult task (Charrad et al., 2014b). Comparison to a multivariate version of preweighted sparse clustering may also be of interest to investigate whether it is more efficient to identify clusters using the sparse version of $\boldsymbol{X}$ or the guided version of $\boldsymbol{Y}$. Finally, there may be more information regarding the disease-subtypes lying in the

within-patient variances and/or longitudinal outcomes. For example, the KmL algorithm was developed to identify clusters from repeated measures (Genolini and Falissard, 2010), and Gaussian mixture models have been used to cluster observations based on differing means and variances (Banfield and Raftery, 1993). These methods may also benefit from feature-guidance prior to applying clustering techniques when the observations are especially noisy.

CHAPTER 4: ESTIMATING INDIVIDUALIZED TREATMENT REGIMES FROM CASE-CONTROL DESIGNS

4.1 Introduction

Finally, we return to the problem setting in which we wish to estimate the optimal individualized treatment regime (ITR) as in Chapter 2, thereby identifying treatment-response subgroups. However, rather than a randomized controlled trial or crossover design, we are now interested in the case-control design where sampling is stratified by disease status. In today's world of rapid technological advances, big data, and electronic health records (EHR), case-control studies have proven to be useful designs to analyze the wealth of information available to us for precision medicine objectives (Adams et al., 2014; Palen et al., 2012; Wu et al., 2010). For example, case-control studies from biobanks, or collections of biological samples, health information, and/or DNA (Olson et al., 2014), and EHRs (Smith et al., 2005) have led to the identification of various genetic biomarkers for elevated risk in coronary heart disease (Keavney et al., 2004), lung cancer (Zhou et al., 2002), and alzheimer's (Khachaturian et al., 2004; Qiu et al., 2004). In this chapter, we propose implementing the generalized outcome weighted learning (GOWL) framework, adjusted by a selection factor, to estimate the optimal ITR from case-control data. This selection factor is principal in accounting for the selection bias inherent in case-control data which are not representative of the total population.

In a case-control study, patients are randomly selected in a stratified manner from disease case and healthy control groups (Armenian, 2009; Keogh and Cox, 2014). Case-control studies are particularly useful in settings where the disease of interest is rare or expensive to study or it is unethical to randomize individuals to the observed treatments being studied (e.g., smoking

status on health outcomes) (Breslow and Day, 1980). Unfortunately, case-control designs have remained widely unexplored as a reasonable option for estimating the optimal ITR, namely because they do not generalize well to the overall population (Breslow, 1996; Glicksberg et al., 2018; Hernán and Robins, 2018).

Consider the Vascular Quality Initiative (VQI) infrainguinal bypass module (Woo et al., 2015) which includes data on over 45,000 patients with peripheral artery disease (PAD), a cardiovascular disease in which patients' narrowed arteries result in reduced blood flow to the limbs, leading to claudication, or discomfort when walking (Hiatt, 2001). PAD may be further complicated in the presence of atherosclerosis, when a buildup of plaque in the blood vessels additionally restrict blood flow (Hirsch et al., 2001). Current guidelines for symptomatic PAD patients undergoing bypass recommend pre-operative antiplatelets and statin drugs (Gerhard-Herman et al., 2017); however, in practice, patients often times receive neither, much less both (Cambou et al., 2010). Thus, it is of interest to identify the optimal ITR among symptomatic PAD patients undergoing bypass to inform clinical recommendations in the case where prescription of only one drug is applicable. A randomized controlled trial may apply here, but data on the disease and treatments of interest are readily available and a cohort or case-control study may be more suitable.

Modifications to Q-learning and outcome weighted learning (OWL) have been made to estimate the optimal ITR from observational data. For example, Moodie et al. (2012) examines methods for eliminating confounding variables for the treatment-effect in the observational setting. Wang et al. (2016) adjust for confounding via propensity scores fit by random forest to handle high-dimensional electronic health record data commonly used for observational studies. However, to our knowledge, no work has been established for estimating the optimal ITR from case-control studies where the study sample may be quite distinct from the total population.

The rest of this chapter is organized as follows. In Section 4.2, we review OWL and generalized outcome weighted learning (GOWL) before introducing the proposed method for case-control studies. We then provide the theoretical properties of the proposed method in Section

4.3. Sections 4.4 and 4.5 present the performance of the proposed estimator through numerical experiments and application to a dataset on cardiovascular disease patients with comparisons to naive and cohort methods.

4.2 Methodology

In this section, we will first review some existing methods for estimating the optimal ITR from a weighted classification standpoint. We then introduce the proposed method, which we will from here refer to as "case-control GOWL."

4.2.1 Existing Methods

Assume we observe i.i.d. data $(\boldsymbol{X}_i, A_i, Y_i)$ for $i = 1, \ldots, n$, from either a randomized clinical trial or an observational cohort study. $A \in \mathcal{A} = \{-1, 1\}$ denotes binary treatment assignment or observed exposure, $\boldsymbol{X} \in \mathcal{X}$ is a p-dimensional vector of covariates, and $Y \in \mathbb{R}$ is a univariate reward, bounded by $M < \infty$, for which greater values are desired. Assume further that Y is of the form

$$Y = \mu(\boldsymbol{X}) + Ac(\boldsymbol{X}) + \epsilon,$$

where $\mu(\boldsymbol{X})$ is a main effect of the covariates, $c(\boldsymbol{X})$ is the treatment-covariate interaction, and ϵ has mean 0 and variance σ_ϵ^2. Note that under this model, the reward is maximized whenever $\text{sign}\{A\} = c(\boldsymbol{X})$. Next, denote $Y^*(a)$ as the counterfactual outcome under treatment a. We then make three causal assumptions (Rubin, 1978) to connect the counterfactual outcomes to the observed data: $P(A = a|\boldsymbol{X}) > 0$ with probability 1, $\{Y^*(1), Y^*(-1)\}$ is independent of A conditional on $\boldsymbol{X}$, and $Y = Y^*(a)$. These are known as positivity, conditional exchangeability, and consistency, respectively.

Formally defined, any ITR, D is a decision rule which maps from the covariates space to the treatment space. The optimal decision rule D_0 is the ITR from the class of all decision rules $\mathcal{D}$

that maximizes the value function (Qian and Murphy, 2011),

$$\mathcal{V}(D) = E\left[\frac{Y1\{A = D(\boldsymbol{X})\}}{P(A|\boldsymbol{X})}\right], \tag{4.1}$$

where $P(A|\boldsymbol{X}) = \Pr(A = a|\boldsymbol{X} = \boldsymbol{x})$ is the propensity score for treatment. Therefore, we may define D_0 as

$$D_0 = \underset{D\in\mathcal{D}}{\operatorname{argmin}}\, E\left[\frac{Y1\{A \neq D(\boldsymbol{X})\}}{P(A|\boldsymbol{X})}\right]. \tag{4.2}$$

OWL views the problem as one of weighted classification, where the class labels are A_i and the weights are Y_i (Zhao et al., 2012). By doing so, support vector machine methods (Cortes and Vapnik, 1995) may be applied by using the hinge loss in place of 0-1 loss in (4.2). Unfortunately, estimates of D_0 from OWL tend to assign patients to their observed A_i when Y_i is negative (Chen et al., 2018; Wang et al., 2016; Zhou et al., 2017), spurring the development of improvements to OWL which better handle negative rewards such as GOWL (Chen et al., 2018). GOWL alternatively uses $|Y_i|$ as the weights and $A_i\text{sign}\{Y_i\}$ as the class labels with a piece-wise hinge loss function.

4.2.2 Case-Control Generalized Outcome Weighted Learning

In a case-control design, n_1 patients are randomly drawn from the control or healthy population, and n_0 patients are randomly drawn from the cases or the diseased population for a total of $n = n_1 + n_0$ in the sample. Because of the stratified sampling in case-control studies, the study sample is not representative of the overall population, particularly in the scenario where the disease is rare (Glicksberg et al., 2018). In some scenarios, n_0 may include all cases from a dataset. Due to the nature of a case-control design, the outcome is binary, i.e., $Y \in \{0, 1\}$. Contrary to popular convention, we will denote cases as $Y = 0$ and controls as $Y = 1$ so that higher values of Y are still desirable. Otherwise, we will retain the same notation from before. Oftentimes, a matched selection process is used whereby patients are matched on some subset of $\boldsymbol{X}$. For the proposed method, matching is not necessary.

Next, let us define $q(\boldsymbol{X})$ and $p(\boldsymbol{X})$ as the density of $\boldsymbol{X}$ in the study sample and the overall population, respectively. Because of selection bias, maximization of (4.1) from the empirical data may not provide a consistent estimator for D_0. Thus, we propose inclusion of a "selection factor," namely $\theta(\boldsymbol{X}) = p(\boldsymbol{X})/q(\boldsymbol{X})$ such that we instead minimize

$$E\left[\frac{|\theta(\boldsymbol{X})Y|}{P(A|\boldsymbol{X})}1\{A \neq D(\boldsymbol{X})\}\right]. \tag{4.3}$$

Under Lemma 4.1, optimization of (4.3) is equivalent to optimization of (4.2); the proof is left to Appendix B.

Lemma 4.1. *Under the given assumptions,*

$$D_0 = \underset{D\in D}{\operatorname{argmin}}\, E_q\left[\frac{\theta(\boldsymbol{X})Y}{P(A_1|\boldsymbol{X})}1\{A_1 \neq D(\boldsymbol{X})\}\right].$$

To estimate D_0, we then minimize the objective function given in (4.4) for $f \in \mathcal{F}$, a reproducing kernel Hilbert space. Here, $\psi(u, v) = \max\{1 - \operatorname{sign}(u)v, 0\}$, λ_n is a tuning parameter, and $||\cdot||$ is the L_2 norm. For details on solving the minimization problem in (4.4), we defer to Chen et al. (2018) and Kimeldorf and Wahba (1970).

$$\underset{f\in\mathcal{F}}{\operatorname{argmin}}\,\frac{1}{n}\sum_{i=1}^{n}\frac{|\theta(\boldsymbol{X}_i)Y_i|}{P(A_{i1}|\boldsymbol{X}_i)}\psi\{Y_i, A_i f(\boldsymbol{X}_i)\} + \lambda_n||f||^2, \tag{4.4}$$

Especially with large p, estimation of $\theta(\boldsymbol{X})$ can be very difficult using typical kernel density estimation (Parzen, 1962; Rosenblatt, 1956; Silverman, 2018). However, by Lemma 4.2, we may more easily estimate $\theta(\boldsymbol{X})$ from estimates of $P(A = a|\boldsymbol{X})$ and $P(Y = y|\boldsymbol{X}, A = a)$, for $a \in \{-1, 1\}$ and $y \in \{0, 1\}$, obtained through regression (e.g., random forests). We further assume knowledge of $P(Y)$, either from previous literature or a representative database. Although selection bias is present in the sample, we may still obtain valid estimates for $P(Y|\boldsymbol{X}, A)$ (Van Der Laan, 2008), and a weighted model for $P(A|\boldsymbol{X})$ may be fit (Walsh et al., 2012). Particularly,

in our implementation with random forests, each individual may be weighted for sampling into each bootstrapped tree.

Lemma 4.2. *Let $r_k = n_k/n$ for $k = 0, 1$. Under the given assumptions,*

$$\theta(\boldsymbol{X}) = \left\{ \sum_{a\in\{-1,1\}} P(A = a|\boldsymbol{X}) \left[\frac{r_0 P(Y = 0|\boldsymbol{X}, A = a)}{P(Y = 0)} + \frac{r_1 P(Y = 1|\boldsymbol{X}, A = a)}{P(Y = 1)} \right] \right\}^{-1}.$$

Thus, we define our estimated decision function as

$$\widehat{f}_n^* = \underset{f\in\mathcal{F}}{\operatorname{argmin}} \frac{1}{n} \sum_{i=1}^{n} \frac{|\widehat{\theta}(\boldsymbol{X}_i)Y_i|}{P(A_i|\boldsymbol{X}_i)} \psi\left\{Y_i, A_i f(\boldsymbol{X}_i)\right\} + \lambda_n ||f||^2, \tag{4.5}$$

and our proposed estimator of the optimal ITR is $\widehat{D}^*(\boldsymbol{X}) = \operatorname{sign}\left\{\widehat{f}_n^*(\boldsymbol{X})\right\}$, where

$$D^* = \underset{D\in\mathcal{D}}{\operatorname{argmin}}\ E\left[\frac{|\theta(\boldsymbol{X})Y|}{P(A|\boldsymbol{X})}\psi\{Y, Af(\boldsymbol{X})\}\right].$$

4.3 Theoretical Results

Let $\mathcal{R}(f) = E[Y\ 1\{A \neq \operatorname{sign}[f(\boldsymbol{X})]\}/P(A|\boldsymbol{X})]$ be the risk under 0-1 loss and $\mathcal{R}_\psi(f) = E\left[\widehat{\theta}(\boldsymbol{X})|Y|\ \psi\left\{Y, Af(\boldsymbol{X})\right\}/P(A|\boldsymbol{X})\right]$ be that under ψ-loss with the estimated adjustment for selection bias. Under Theorem 4.1, we have Fisher consistency for $D^*(\boldsymbol{X}) = \operatorname{sign}\{f^*(\boldsymbol{X})\}$, where $f^*(\boldsymbol{X}) = \operatorname{argmin}_{f\in\mathcal{F}} \mathcal{R}_\psi(f)$.

Theorem 4.1. *Under the given assumptions, $D^*(\boldsymbol{X}) = D_0(\boldsymbol{X})$.*

Next, let $\overline{\mathcal{F}}$ be the closure of $\mathcal{F}$ and f_0 and f_0^* be the minimizers of $\mathcal{R}(f)$ and $\mathcal{R}_\psi(f)$, respectively, over all functions f. Theorem 4.2 then provides us with global consistency.

Theorem 4.2. *Let $\lambda_n > 0$ be a sequence such that $\lambda_n \to 0$ and $\lambda_n n \to \infty$ with probability going to 1 as $n \to \infty$. For any distribution P of $(\boldsymbol{X}, A, \boldsymbol{Y})$, $\lim_{n\to\infty} \mathcal{R}_\psi(\widehat{f}_n^*) \to_P \mathcal{R}_\psi(f^*)$. Furthermore, $\lim_{n\to\infty} \mathcal{R}(\widehat{f}_n^*) \to_P \mathcal{R}(f_0)$ whenever $f_0^* \in \overline{\mathcal{F}}$.*

4.4 Numerical Experiments

To demonstrate the performance of the proposed method, we present results from a set of simulations. The covariates were generated as 50 i.i.d. variables from a $U(-1, 1)$ distribution. A was sampled from $\{-1, 1\}$ with probability $\text{expit}\{3(1 + X_1 + X_2)\}$ of being 1. Y was sampled with probability $\text{expit}\{5 - X_1 - 2X_2 + X_3 + 5A[1 + 3(X_1 + X_2)]\}$ from a binomial distribution. A population dataset of size $n_{\text{pop}} = 100,000$ was generated. Under the data generation described, the population dataset contained a 9.1% prevalence of cases. The allocation of the true optimal ITR, i.e. $\text{sign}\{1 + 3(X_1 + X_2)\}$, was 34.7% to $A = -1$ and 65.3% to $A = 1$. Simulations were repeated 1,000 times each, varying the sample size of the study dataset across $n = 50, 100, 200, 500, 1000$ where cases and controls were sampled at a 1:1 ratio.

A random forest was fit for $P(Y|\boldsymbol{X}, A)$ and a weighted random forest was fit for $P(A|\boldsymbol{X})$ (Breiman, 2001; Ishwaran et al., 2008) using the randomForestSRC R package (Ishwaran and Kogalur, 2007), cases were weighted by $P(Y = 0)$ and controls were weighted by $P(Y = 1)$. $P(Y)$ was assumed to be known from the population dataset. The proposed method was compared to the "naive" approach in which a case-control sample is analyzed but there is no correction for selection bias. A "cohort" method was also performed for comparison in which data of size $2n$ were randomly sampled from the population dataset. For all methods, GOWL was performed using the DynTxRegime package in R, version 3.4.1 (Holloway et al., 2018; R Core Team, 2017). The kernel was correctly specified to be linear, and λ_n was selected from the grid $[0.1, 0.5, 1, 5, 10, 50, 100, 500]/n$ via 5-fold cross validation.

Figure 4.1 displays the average classification accuracy and

$$\frac{\mathbb{P}_{n_{\text{pop}}}[Y1\{A = \widehat{D}^*(\boldsymbol{X})\}]/P(A|\boldsymbol{X})}{\mathbb{P}_{n_{\text{pop}}}[1\{A = \widehat{D}^*(\boldsymbol{X})\}/P(A|\boldsymbol{X})]},$$

the estimated mean value (Qian and Murphy, 2011) where $\mathbb{P}_n$ is the empirical mean. At smaller sample sizes, the proposed and naive methods perform similarly in accuracy, with some advantage over the cohort method. With larger n, however, the proposed method performs somewhere

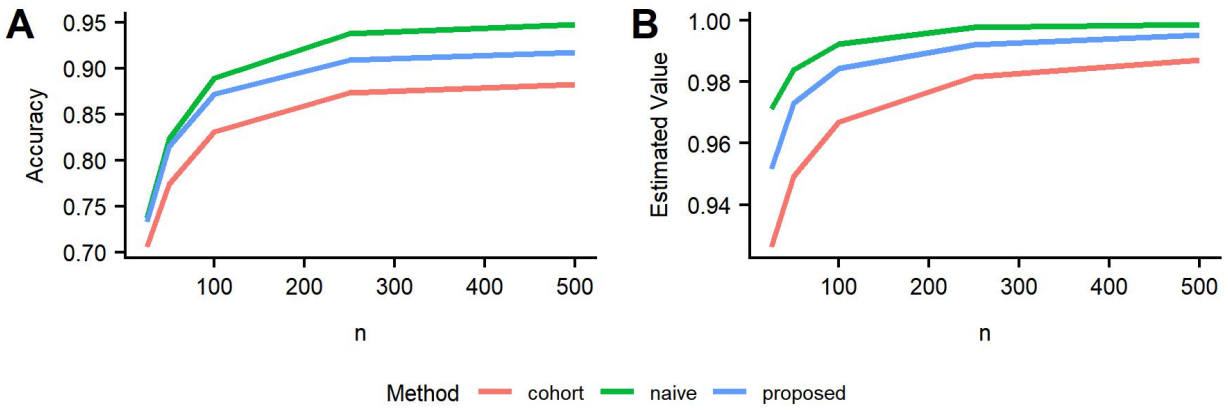

Figure 4.1: Average classification accuracy (A) and estimated value (B) across 1,000 replications at each sample size n in simulation.

between the naive and cohort approaches in terms of classification accuracy. The estimated value for the three methods appear to be parallel as n increases, with the proposed method performing somewhere in between the naive and cohort methods. These results show promise for the proposed method at certain sample sizes, although the exact scenario in which the proposed method will greatly outperform the others is still unclear. We believe the data generation mechanism must produce data which are sufficiently different in $p(\boldsymbol{X})$ and $q(\boldsymbol{X})$ while maintaining a reasonable difference in treatment effect.

Results on the mean square error (MSE) across all simulations are provided in Table 4.1 for estimating $\theta(\boldsymbol{X})$. Although the estimates decrease with n, the rate of convergence toward 0 may be of concern. These results merit further investigation into the algorithm for estimating $\theta(\boldsymbol{X})$. It is known that tree-based methods produce non-smooth estimates (Friedman et al., 2001); in the future, we may instead use a different regression technique such as multivariate adaptive regression splines (Friedman, 1991).

Table 4.1: Mean (sd) mean square error for estimating $\theta(\boldsymbol{X})$.

n	50	100	200	500	1000
MSE	0.44 (0.07)	0.52 (0.05)	0.38 (0.04)	0.34 (0.02)	0.31 (0.02)

4.5 Treatment Subgroups for Peripheral Artery Disease

Over 200 million people worldwide have peripheral artery disease (PAD) including estimates of between 8 and 12 million people in the United States alone (Mozaffarian et al., 2015). PAD disproportionately affects older adults, including up to 20% of those aged 65 and older in the US. Significant individual- and health care system-level consequences result if PAD is not managed appropriately (Hirsch et al., 2008). Much of the burden is preventable by way of modifiable risk factors such as diabetes and smoking (Gerald R. Fowkes et al., 1992; Kannel, 1973; Muntner et al., 2005; Navas-Acien et al., 2004; Selvin et al., 2006; Wattanakit et al., 2005). Poor risk factor management causes adverse events including limb- and life-threatening sequelae (Dormandy, 2000). As guidelines for PAD have been implemented, evaluation of adherence to these recommendations have shown reductions of adverse events by nearly 50% (Armstrong et al., 2014). Thus, there is tremendous benefit to using evidence-based practices in the management of PAD in order to limit downstream morbidity and mortality and associated health care costs.

The American College of Cardiology/American Heart Association (AHA/ACC) release updated guidelines on managing lower extremity PAD (Gerhard-Herman et al., 2017) every five years. These guidelines provide a "Class of Reccomendation" that is meant to describe the "magnitude and certainty of benefit in proportion to risk" where Class I recommendations are considered best practices meant to indivate true guideline-directed management and therapy. Guidelines are unique to patients believed to be at risk for PAD, those with symptomatic PAD being medically managed, and those being considered for revascularization. Among patients being considered for/undergoing revascularization, Class I recommendations define best practices for medical management, imaging methods to assess anatomy, and specific operative techniques. All patients undergoing surgical bypass should receive antiplatelet (e.g., aspirin) and statin therapy to reduce the risk of subsequent major adverse events. However, many are not prescribed one or either in real world practice, and patterns often stray from the recommended guidelines (Cambou et al., 2010). It is compelling to consider the combination of these treatments and whether patients may

benefit from receiving antiplatelet or statin drugs alone. Therefore, a precision medicine approach could be helpful in identifying the relevant treatment-subgroups of PAD to reduce the occurrence of adverse events..

The Vascular Quality Intiative (VQI) was designed to improve the quality, safety, effectiveness, and cost of vascular helath care. As of January 2019, the VQI has 536 participating centers and includes 5,215 physicians. The VQI infrainguinal bypass module was used to identify adult patients (≥ 18 years) who underwent bypass for symptomatic PAD between 2007 and 2018. Primary outcomes included major adverse limb events (MALE), ipsilateral amputation and mortality. MALE includes those returning to the operating room for thrombosis, thrombectomy/lysis revision of the graft, graft failure, or ipsilateral major limb amputation. Patients may be prescribed a statin, antiplatelets, neither, or a combination treatment prior to the bypass procedure. The outcome Y was coded to be a case if any of the aforementioned adverse events occurred. Covariates included in the model were diabetes, gender, age, prior history of coronary heart failure (CHF), chronic obstructive pulmonary disease (COPD), dialysis, and living status (home, nursing home, or homeless).

Case-control GOWL was fit alongside the naive case-control and cohort methods, with $n = 500$. A linear kernel was used in all methods, searching the grid $[0.1, 0.51, 5, 10, 50, 100, 500]/n$ for λ_n in 10-fold cross validation. The dataset was constrained to the $9,716$ patients receiving only one of the two treatments, and patients were selected via stratified sampling for the case-control methods at a 1:1 ratio and via random sampling with equal probability for the cohort method. The observed value in the constrained dataset was 38.50%, i.e., we observed 38.50% of individuals to have an adverse event occur. The estimated value following the estimated optimal ITR from case-control GOWL was 36.67%, while that from the naive and cohort methods were 37.16% and 37.50%, respectively. Although all methods lead to rather marginal improvements on the observed prevalence, the proposed method leads to the greatest decrease in the prevalence of adverse events.

Table 4.2 provides the proportional make up or average of covariates in each subgroup, as observed in the dataset and among those who followed the case-control GOWL estimated optimal ITR. In the observed dataset, those prescribed statin did not greatly differ from those prescribed antiplatelets; however, 54% of those prescribed statin were diabetic compared to 39% of those prescribed antiplatelets. In contrast, according to the estimated optimal ITR, the subgroup for which statin is recommended over antiplatelets were older and contained a much larger proportion of females, diabetics, and individuals with history of CHF and/or COPD. The statin subgroup also had a slightly different proportion of patients on dialysis, in nursing homes, or who were homeless.

Table 4.2: Proportional make up for each subgroup or mean (sd) for age.

	Case-Control GOWL		Observed	
	Antiplatelets	Statin	Antiplatelets	Statin
Age (years)	56.69 (7.85)	73.84 (7.38)	66.70 (11.89)	67.49 (10.75)
Female	0.18	0.37	0.68	0.68
Diabetes	0.38	0.55	0.39	0.54
CHF	0.04	0.24	0.14	0.16
COPD	0.13	0.36	0.25	0.28
Dialysis	0.06	0.09	0.07	0.07
Home Living	0.97	0.97	0.96	0.96
Nursing Home Living	0.02	0.03	0.04	0.03
Homeless	0.01	< 0.01	< 0.01	< 0.01

Results from this analysis corroborate the findings from other studies such as Mortensen et al. (2016) that statin drugs performed better in reducing the number of cardiovascular disease events in individuals with increased levels coronary artery calcium and carotid plaque burden, risk factors for coronary heart failure and comorbidities with diabetes and dialysis. Targetting treatment of PAD patients with statin or antiplatelets is a first step in minimizing adverse events. Future work should confirm these findings and investigate on the effects of combination therapy in comparison to statin or antiplatelet drugs only.

4.6 Discussion

In this chapter, we have proposed a weighted classifier for estimating the optimal ITR from case-control data. The classifier accounts for selection bias in the form of a selection factor, $\theta(\boldsymbol{X})$, which may easily be estimated from the study sample using regression methods. The estimator is simple to implement using the existing R packages, and, in simulation, competes well with the naive estimator. Case-control GOWL can perform well in some real world settings, such as the PAD example given in this chapter.

Case-control GOWL stands to show improvement both in simulation and in the real data setting, however. Further numerical experiments where $p(\boldsymbol{X})$ and $q(\boldsymbol{X})$ are sufficiently different are necessary to observe the potential in accuracy and estimated value gains that case-control GOWL may have over the naive method. Furthermore, simulation scenarios varying rarity of the outcome and with more complicated treatment-covariate interactions (solved by a Gaussian kernel) are necessary, as case-control studies are not always in the setting of rare outcomes or linear treatment-covariate interactions. Finally, both the numerical experiments and analysis on PAD patients were limited in computational performance. Increasing the sample size became computationally inefficient, and, with smaller sample sizes, an issue of computational singularity could occur quite often. This is typically due to limitations in R regarding its quadratic solver. Attempting the analysis in Python would be of interest, particularly with multiple replications in the PAD analysis to assess the stability of the results.

Aside from the aforementioned future steps, there are several extensions on the proposed method that may be explored. For example, the proposed method considers only binary treatment options. In the case of more than 2 treatment options, a series of binary classifiers may be implemented (Dietterich and Bakiri, 1994). In the PAD example discussed here, we may next compare the combination of treatments, statin and antiplatelets, to the optimal option between statin and antiplatelets alone. Alternatively, a single multi-category classifier may be used, as in multi-category support vector machines (Lee et al., 2004; Liang et al., 2018; Zhu et al., 2004).

Additionally, the residual from fitting a model for $E[Y|X]$ may be used in place of Y in the classifier, as proposed by Fu et al. (2016) and Zhou et al. (2017), who have seen favorable results using residual weights. Finally, methods such as those suggested by Chen et al. (2018), Song et al. (2015), Xu et al. (2015), and Zhou et al. (2017) may be incorporated for variable selection, e.g., an L_1 penalty could be imposed during optimization to simultaneously restrict model complexity and perform variable selection.

CHAPTER 5: DISCUSSION AND FUTURE RESEARCH

With advancements in medicine, the need for precision medicine has become abundantly clear. Diseases and treatment-response may present with great heterogeneity from patient to patient, and a "one size fits all" approach can no longer be considered appropriate in all situations. This dissertation presents work to expand pre-existing methodology into new frameworks to make more efficient use of the data that investigators collect or have already collected. Chapters 2 and 4 discuss bringing generalized outcome weighted learning, a weighted classification technique, into the realms of two study designs that have been, to date, unexplored for ITR estimation. The theoretical groundwork for these methods have been laid, and the method for crossover studies appears to perform well in comparison to competing methods. While the method proposed in Chapter 4 has greater room for improvement, current simulations and application to a dataset on peripheral artery disease patients show promising results in comparison to the naive method. Lastly, we proposed a novel clustering technique in Chapter 3 which we believe may be incorporated with nearly any pre-existing method wherein the variables are believed to contain a high degree of noise. The method performs quite well in simulation, and the resulting clusters from application to SEARCH for Diabetes in Youth cohort 1 visit data revealed clinically meaningful separation of individuals, both in weight-glycemia phenotypic differences and demographic differences. We now discuss the current and future challenges ahead; next steps for the work presented in this dissertation to take in the months or years to come.

As mentioned in Section 2.6, there are a number of potential extensions for estimating the ITR from a crossover study. One of the largest drawbacks of all OWL techniques is the restriction to two treatment arms. Liang et al. (2018) propose using an outcome weighted deep learning

method to consider, not only multiple treatment arms, but also cross-arm combinations of treatments. With proper adjustment for carryover effects, the concepts from outcome weighted deep learning and the crossover design could together be very powerful in estimating ITRs from a variety of settings. This extension would additionally address another drawback to crossover GOWL by being able to consider data from a crossover study with more than 2 periods and more than 2 treatments. Eventually, such work could also lead to application to cluster randomized trials and longitudinal study designs. Further simulations may also be considered with more scenarios and comparison methods. For example, scenarios in which $c(\boldsymbol{X})$ contain complex interactions or extreme non-linearity are of interest for comparison.

While the numerical experiments presented in Section 3.3 shows promise, further simulations are required to examine the effect of varying the noise in both $\boldsymbol{X}$ and $\boldsymbol{Y}$. Comparison to clustering on $\boldsymbol{X}$ alone and $\boldsymbol{X}$ and $\boldsymbol{Y}$ together would provide additional evidence to the validity of the proposed method. Finally, comparisons to other semi-supervised clustering methods, such as preweighted sparse clustering (Gaynor and Bair, 2017), are of interest. However, at the present time, R packages for such methods are still in preparation.

The clustering method proposed in Chapter 3 may be continue to be explored in a variety of contexts. For example, application to categorical, repeated measure, or ordinal outcomes would prove the versatility of the proposed method. Additionally, we may explore the potential gains from using other clustering methods such as combinatorial or mixture model methods. Lastly, it is of interest to revisit the original idea, as presented in the preliminary dissertation document, wherein the variance and correlation estimates of the outcomes are included as cluster variables. The results from Chapter 3 are encouraging, but the proper scenario in which clustering on the variance and correlation estimates in addition to the mean estimates remains unclear.

Similarly, the setting in which the estimator proposed in Chapter 4 will exhibit significant gains over other methods also remains unclear. We believe the density of $\boldsymbol{X}$ must differ greatly between the sample and true populations, but the data propagation technique to do so while maintaining a reasonable treatment effect has proven difficult thus far. In the future, we hope to inves-

tigate this issue alongside the performance of the estimation technique for $\theta(\boldsymbol{X})$. Again, application to multiple treatments, like that proposed by Liang et al. (2018), would prove highly useful. For example, with the data on symptomatic PAD patients, we may further research into whether the combination of antiplatelet and statin drugs can reduce the overall prevalence of adverse events compared with either of the drugs alone. Other improvements on the proposed method include considering multiple treatments and decision time points. Additionally, BOWL and SOWL (Zhao and Zeng, 2013) have been developed as extensions of OWL to estimate a sequence of decisions as the optimal ITR. With the wealth of data available with EHRs and biobanks, methods to combine case-control GOWL with BOWL or SOWL could become powerful tools in estimating the multiple time point optimal ITR.

Finally, the simulations performed in Chapters 2 and 4 were greatly limited by the poor quadratic solver in R version 3.4.1 (R Core Team, 2017). Other software in programming languages such as Python and MATLAB are known to have more efficient solvers with fewer problems of singularity. Reprogramming the simulations in one of these languages may provide great improvements in the computational efficiency.

APPENDIX A: TECHNICAL DETAILS FOR CHAPTER 2

Clinical Details for the FAME Estimated ITR

92% of study participants, $(n = 49)$ were assigned to the HFLS diet according to crossover GOWL to maximize change in fullness from baseline. To characterize the subgroup that, on average, experiences a larger increase in patient reported fullness, Figure A.1 displays the distribution of continuous features across the estimated subgroups. Those assigned to the HFLS diet tend to be older with higher A1c. Because the HSLF group is small ($n = 4$), two-sample t-tests would not be appropriate to test for significant differences between groups, and trends observed in Figure A.1 should be confirmed in future studies. However, sex $(p = 0.1131)$, ethnicity $(p = 1)$, and Tanner stage $(p = 0.4427)$ were tested using Fisher's exact tests. All tests were non significant at the 0.05 level.

Figure A.1 also displays the distribution of continuous features across the estimated subgroups to minimize the change in hunger from baseline. 51% $(n = 27)$ of participants were assigned to HFLS. Those assigned to HFLS tend to be older, but differences in other covariates are not apparent. Although the sample in the HSLF is larger when we consider hunger as the outcome, both samples are still rather small. For this reason, two-sample t-tests are still not appropriate. Fisher's exact tests again did not yield any significant differences in sex $(p = 0.5857)$, ethnicity $(p = 1)$, or Tanner stage $(p = 0.7040)$.

In conclusion, using crossover GOWL appears to be effective for estimating the optimal ITR to maximize the change in satiety. Future research should confirm these subgroups in large sample sizes to better compare differences across features. If verified, future recommendations for adolescent minorities can be tailored by age and A1c levels to improve weight loss. Studies on overweight and obese minority adolescents are still needed to research alternative interventions for those that report feeling more satiated from the typical Western diet (HSLF).

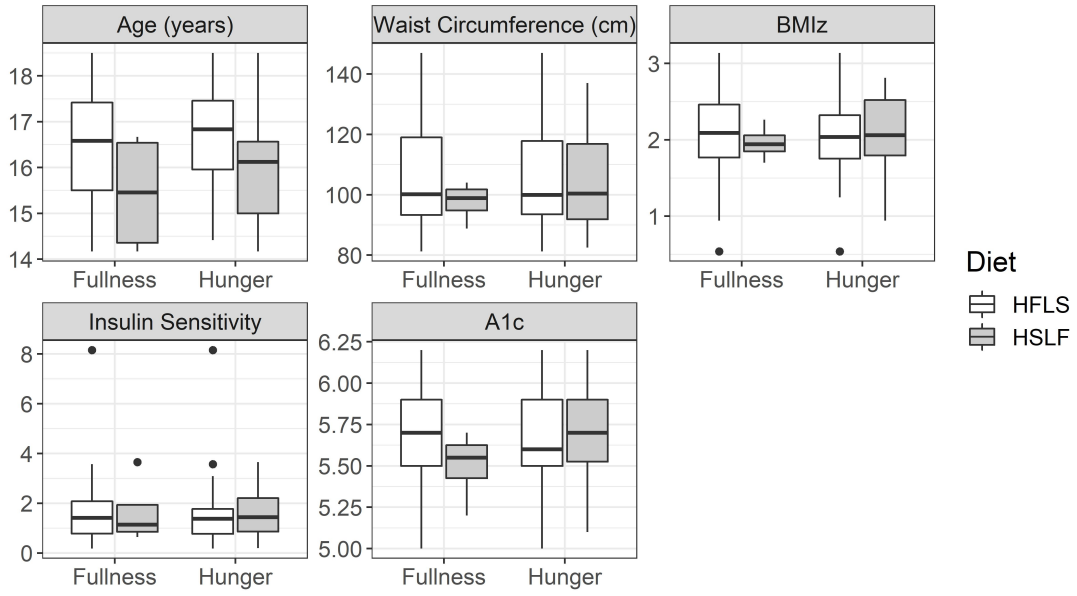

Figure A.1: Distribution of features across the crossover GOWL estimated diet-outcome subgroups for both fullness and hunger outcomes

Theoretical Details for Crossover GOWL

A.0.1 Assumptions

The following assumptions are made for the theory behind the method proposed in Chapter 2.

1. *Positivity*: $P(A_1 = a|\boldsymbol{X} = \boldsymbol{x}) \geq \pi_0 > 0$ with probability 1

2. *Conditional Exchangeability*: $\{Y^*(-1), Y^*(1)\} \perp A_1|\boldsymbol{X}$

3. *Consistency*: $Y_k = Y^*(a_k) - \delta_{A_1}(\boldsymbol{X})1\{k = 2\}$

4. Outcomes follow the model

$$Y_k = \mu(\boldsymbol{X}) + A_k c(\boldsymbol{X}) + \delta_{A_1}(\boldsymbol{X})1\{k = 2\} + \epsilon_k,$$

for periods $k = 1, 2$. $\boldsymbol{\epsilon} = (\epsilon_1, \epsilon_2)^\top$ has a semi-definite covariance matrix, Σ_ϵ.

5. There exist $M_0, M_1 < \infty$ such that $|Y_k| < M_0$ almost surely, $|\delta_{A_1}(\boldsymbol{X})| < M_1$ almost surely, and $P\left(|\widehat{\delta}_{A_1}(\boldsymbol{X})| < M_1\right) \to 1$ as $n \to \infty$

6. $\mathbb{P}\left[1\{\text{sign}[\widehat{R}] \neq \text{sign}[R]\}\right] = o_P(\lambda_n)$

A.0.2 Proof of Lemma 2.1

The optimal ITR is $D_0 = \text{argmax}_{D\in\mathcal{D}} E[Y^*\{D(\boldsymbol{X})\}]$. Note that, under Assumption (4), $D_0(\boldsymbol{X}) = \text{sign}\{c(\boldsymbol{X})\}$. The expected treatment response difference between treating according to D_0 and treating opposite to D_0 is

$$\begin{aligned} E\left[Y^*\{D_0(\boldsymbol{X})\} - Y^*\{-D_0(\boldsymbol{X})\}\right] &= E[Y^*\{\text{sign}[c(\boldsymbol{X})]\} - Y^*\{-\text{sign}[c(\boldsymbol{X})]\}] \\ &= 2|c(\boldsymbol{X})| \\ &\geq E[Y^*\{D(\boldsymbol{X})\} - Y^*\{-D(\boldsymbol{X})\}], \end{aligned}$$

for all $D \in \mathcal{D}$. Thus, the optimal ITR also maximizes the treatment-response difference, or $D_0 = \text{argmax}_{D\in\mathcal{D}} E[Y^*\{D(\boldsymbol{X})\} - Y^*\{-D(\boldsymbol{X})\}]$. Therefore, it can be seen that

$$\begin{aligned} D_0 &= \underset{D\in\mathcal{D}}{\text{argmax}}\, E\left[\{Y^*(1) - Y^*(-1)\}D(\boldsymbol{X})\right] \\ &= \underset{D\in\mathcal{D}}{\text{argmax}}\, E\left[\frac{1\{A_1 = D(\boldsymbol{X})\}}{P(A_1|\boldsymbol{X})}\left[Y_1 - Y_2 + \delta_{A_1}(\boldsymbol{X})\right]\right. \\ &\quad \left. + \frac{1\{A_1 \neq D(\boldsymbol{X})\}}{P(A_1|\boldsymbol{X})}[Y_2 - \delta_{A_1}(\boldsymbol{X}) - Y_1]\right] \\ &= \underset{D\in\mathcal{D}}{\text{argmin}}\, E\left[\frac{Y_1 - Y_2 + \delta_{A_1}(\boldsymbol{X})}{P(A_1|\boldsymbol{X})}\, 1\{A_1 \neq D(\boldsymbol{X})\}\right] \\ &= \underset{D\in\mathcal{D}}{\text{argmin}}\, E\left[\frac{R}{P(A_1|\boldsymbol{X})}\, 1\{A_1 \neq D(\boldsymbol{X})\}\right], \end{aligned}$$

where the second equality follows from Assumption (3). This proves the result.

A.0.3 Proof of Theorem 2.1

This proof follows from Lemma 2.1 and results from Lin (2002). Recall that $\psi(u, v) = \max\{1 - \text{sign}(u)v, 0\}$. Minimizing the risk, $\mathcal{R}_\psi(f)$ is equivalent to minimizing the conditional risk,

$$\mathcal{R}_\psi(f, \boldsymbol{x}) = E\left[\frac{|R|}{P(A_1|\boldsymbol{X})}\psi\{R, A_1 f(\boldsymbol{X})\}\Big|\boldsymbol{X} = \boldsymbol{x}\right],$$

for every fixed $\boldsymbol{x} \in \mathcal{X}$. Let $R^+ = R1\{R \geq 0\}$ and $R^- = R1\{R < 0\}$. By the law of total expectation, the conditional risk becomes

$$\begin{aligned}
\mathcal{R}_\psi(f, \boldsymbol{x}) &= E\left[|R|\ \psi\{R, f(\boldsymbol{X})\}\Big|\boldsymbol{X} = \boldsymbol{x}, A_1 = 1\right] + E\left[|R|\ \psi\{R, -f(\boldsymbol{X})\}\Big|\boldsymbol{X} = \boldsymbol{x}, A_1 = -1\right] \\
&= E\left[R^+ \max\{1 - f(\boldsymbol{X}), 0\} - R^- \max\{1 + f(\boldsymbol{X}), 0\}\Big|\boldsymbol{X} = \boldsymbol{x}, A_1 = 1\right] \\
&\quad + E\left[R^+ \max\{1 + f(\boldsymbol{X}), 0\} - R^- \max\{1 - f(\boldsymbol{X}), 0\}\Big|\boldsymbol{X} = \boldsymbol{x}, A_1 = -1\right].
\end{aligned}$$

Next, note that $\mathcal{R}_\psi\{\text{sign}(f), \boldsymbol{x}\} < \mathcal{R}_\psi(f, \boldsymbol{x})$ whenever $f(\boldsymbol{x}) \notin [-1, 1]$. For example, when $f(\boldsymbol{x}) < -1$, the conditional risk reduces to

$$[1 - f(\boldsymbol{x})]\left\{E\left[R^+\Big|\boldsymbol{X} = \boldsymbol{x}, A_1 = 1\right] - E\left[R^-\Big|\boldsymbol{X} = \boldsymbol{x}, A_1 = -1\right]\right\},$$

which is monotonically increasing as $f(\boldsymbol{x}) \to -\infty$. A similar argument is made for when $f(\boldsymbol{x}) > 1$. Thus, we restrict our search to $f(\boldsymbol{x}) \in [-1, 1]$. Then,

$$\begin{aligned}
\mathcal{R}_\psi(f, \boldsymbol{x}) &= E\left[R^+ - R^-\Big|\boldsymbol{X} = \boldsymbol{x}, A_1 = 1\right] + E\left[R^+ - R^-\Big|\boldsymbol{X} = \boldsymbol{x}, A_1 = -1\right] \\
&\quad + f(\boldsymbol{X})\left\{-E\left[R^+ - R^-\Big|\boldsymbol{X} = \boldsymbol{x}, A_1 = 1\right] + E\left[R^+ + R^-\Big|\boldsymbol{X} = \boldsymbol{x}, A_1 = -1\right]\right\} \\
&= E\left[|R|\Big|\boldsymbol{X} = \boldsymbol{x}, A_1 = 1\right] + E\left[|R|\Big|\boldsymbol{X} = \boldsymbol{x}, A_1 = -1\right] \\
&\quad + f(\boldsymbol{X})\left\{E\left[R\Big|\boldsymbol{X} = \boldsymbol{x}, A_1 = -1\right] - E\left[R\Big|\boldsymbol{X} = \boldsymbol{x}, A_1 = 1\right]\right\}.
\end{aligned}$$

If $f^*(\boldsymbol{x})$ minimizes the conditional risk, then $f^*(x)$ must have the sign opposite of the expression $E\left[R\middle|\boldsymbol{X}=\boldsymbol{x}, A_1=-1\right]-E\left[R\middle|\boldsymbol{X}=\boldsymbol{x}, A_1=1\right]$, and thus $D_0(\boldsymbol{X})=\text{sign}\{f^*(\boldsymbol{X})\}$

A.0.4 Proof of Theorem 2.2

First, define the loss functions

$$L_\psi(f)=\frac{|R|}{P(A_1|\boldsymbol{X})}\psi\{R, A_1 f(\boldsymbol{X})\}$$

and

$$\widehat{L}_\psi(f)=\frac{\left|\widehat{R}\right|}{P(A_1|\boldsymbol{X})}\psi\{\widehat{R}, A_1 f(\boldsymbol{X})\}.$$

Next, we show that $||\widehat{f}_n^*||$ is bounded. For any $f\in\overline{\mathcal{F}}$,

$$\mathbb{P}_n\widehat{L}_\psi(\widehat{f}_n^*)+\lambda_n||\widehat{f}_n^*||^2\leq\mathbb{P}_n\widehat{L}_\psi(f)+\lambda_n||f||^2,$$

by definition of $\widehat{f}_n^*$. If we choose $f=0$, then, for all n large enough,

$$\begin{aligned}\mathbb{P}_n\widehat{L}_\psi(\widehat{f}_n^*)+\lambda_n||\widehat{f}_n^*||^2&\leq\mathbb{P}_n\widehat{L}_\psi(0)+\lambda_n||0||^2\\&=\mathbb{P}_n\left\{\frac{|\widehat{R}_i|}{P(A_{i,1}|\boldsymbol{X}_i)}\right\}\\&\leq\pi_0^{-1}(2M_0+M_1),\end{aligned}$$

where the last inequality holds because of Assumptions (1), (5), and (6). Define $M=\pi_0^{-1}(2M_0+M_1)<\infty$. Then, because $\mathbb{P}_n\widehat{L}_\psi(\widehat{f}_n^*)\geq 0$, we have that $\lambda_n||\widehat{f}_n^*||^2\leq M$.

For any bounded f, such as $\widehat{f}_n^*$, we may show that $\left|\mathbb{P}_n\left\{L_\psi(f)-\widehat{L}_\psi(f)\right\}\right|=o_P(1)$:

$$
\begin{aligned}
\left|\mathbb{P}_n\left\{L_\psi(f)-\widehat{L}_\psi(f)\right\}\right| &\le \mathbb{P}\left|L_\psi(f)-\widehat{L}_\psi(f)\right| + o_P(1)\\
&\le \pi_0^{-1}\mathbb{P}\left||R|\psi\{R,A_1f(\boldsymbol{X})\}-|\widehat{R}|\psi\left\{\widehat{R},A_1f(\boldsymbol{X})\right\}\right| + o_P(1)\\
&\le \pi_0^{-1}\mathbb{P}\left|\max\{|R|,|\widehat{R}|\}\left[\psi\{R,A_1f(\boldsymbol{X})\}-\psi\left\{\widehat{R},A_1f(\boldsymbol{X})\right\}\right]\right| + o_P(1)\\
&\le \pi_0^{-1}(2M_0+M_1)\mathbb{P}\left|\psi\{R,A_1f(\boldsymbol{X})\}-\psi\left\{\widehat{R},A_1f(\boldsymbol{X})\right\}\right| + o_P(1)\\
&\le 2M(\pi_0\lambda_n)^{-1}(2M_0+M_1)\mathbb{P}\left|1\{\mathrm{sign}[R]\neq\mathrm{sign}[\widehat{R}]\}\right| + o_P(1)\\
&= 2M^2\lambda_n^{-1}o_P(\lambda_n)+o_P(1)\\
&= o_P(1)
\end{aligned}
$$

Next, we have

$$
\begin{aligned}
\mathbb{P}_nL_\psi(\widehat{f}_n^*) &= \mathbb{P}_nL_\psi(\widehat{f}_n^*)+\mathbb{P}_n\widehat{L}_\psi(\widehat{f}_n^*)-\mathbb{P}_n\widehat{L}_\psi(\widehat{f}_n^*)\\
&\le \mathbb{P}_n\widehat{L}_\psi(\widehat{f}_n^*)+\left|\mathbb{P}_n\left\{L_\psi(\widehat{f}_n^*)-\widehat{L}_\psi(\widehat{f}_n^*)\right\}\right|+\lambda_n||\widehat{f}_n^*||^2\\
&\le \mathbb{P}_n\widehat{L}_\psi(f^*)+\lambda_n||f^*||^2+\left|\mathbb{P}_n\left\{L_\psi(\widehat{f}_n^*)-\widehat{L}_\psi(\widehat{f}_n^*)\right\}\right|\\
&\le \mathbb{P}_nL_\psi(f^*)+\lambda_n||f^*||^2+\left|\mathbb{P}_n\left\{L_\psi(\widehat{f}_n^*)-\widehat{L}_\psi(\widehat{f}_n^*)\right\}\right|+\left|\mathbb{P}_n\left\{L_\psi(f^*)-\widehat{L}_\psi(f^*)\right\}\right|.
\end{aligned}
$$

Taking the $\limsup$ on both sides, we find

$$
\limsup_{n\to\infty}\mathbb{P}_nL_\psi(\widehat{f}_n^*)\le\mathbb{P}L_\psi(f^*)+o_P(\lambda_n)\le\mathbb{P}L_\psi(\widehat{f}_n^*)+o_P(\lambda_n)
$$

Thus, it suffices to show that $\mathbb{P}_nL_\psi(\widehat{f}_n^*)-\mathbb{P}L_\psi(\widehat{f}_n^*)\to_P 0$. Because $\lambda_n||\widehat{f}_n^*||^2$ is bounded by M, $\{\sqrt{\lambda_n}f:||\sqrt{\lambda_n}f||\le\sqrt{M}\}$ is contained in a Donsker class. Note that $\psi(u,v)$ is Lipschitz continuous with respect to v, and, thus, $L_\psi(f)$ is Lipschitz continuous with respect to f. Therefore, $\{\sqrt{\lambda_n}L_\psi(f):||\sqrt{\lambda_n}f||\le\sqrt{M}\}$ is also Donsker. This gives us $\sqrt{n\lambda_n}\{\mathbb{P}_n-\mathbb{P}\}L_\psi(\widehat{f}_n^*)=O_p(1)$, which implies $\{\mathbb{P}_n-\mathbb{P}\}L_\psi(\widehat{f}_n^*)=o_P(1)$. We finally arrive at $\left|\mathcal{R}_\psi(f^*)-\mathcal{R}_\psi(\widehat{f}_n^*)\right|=o_P(1)$.

Furthermore, when $f_0^* \in \overline{\mathcal{F}}$, $f_0^* = f^*$, and

$$\left|\mathcal{R}(\widehat{f}_n^*) - \mathcal{R}(f_0)\right| \leq \left|\mathcal{R}_\psi(\widehat{f}_n^*) - \mathcal{R}_\psi(f_0^*)\right| = o_P(1),$$

where the first inequality holds from Bartlett et al. (2006).

APPENDIX B: TECHNICAL DETAILS FOR CHAPTER 4

Assumptions

The following assumptions are made for case-control GOWL.

1. *Positivity*: $P(A = a)|\boldsymbol{X} = \boldsymbol{x}) > 0$ with probability 1
2. *Conditional Exchangeability*: $\{Y^*(-1), Y^*(1)\} \perp A|\boldsymbol{X}$
3. *Consistency*: $Y = Y^*(a_k)$
4. Outcomes follow the model

$$Y = \mu(\boldsymbol{X}) + Ac(\boldsymbol{X}) + \epsilon,$$

where ϵ has variance σ_ϵ^2

Proof of Lemma 4.1

Note that the optimal ITR may be expressed as

$$\begin{aligned}
D_0 &= \underset{D\in\mathcal{D}}{\operatorname{argmin}} E\left[\frac{Y}{P(A|\boldsymbol{X})}1\{A \neq D(\boldsymbol{X})\}\right] \\
&= \underset{D\in\mathcal{D}}{\operatorname{argmin}} \int_{\mathcal{X}} p(\boldsymbol{X}\frac{Y}{P(A|\boldsymbol{X})}1\{A \neq D(\boldsymbol{X})\}d\boldsymbol{X} \\
&= \underset{D\in\mathcal{D}}{\operatorname{argmin}} \int_{\mathcal{X}} \frac{q(\boldsymbol{X})}{q(\boldsymbol{X})}p(\boldsymbol{X})\frac{Y}{P(A|\boldsymbol{X})}1\{A \neq D(\boldsymbol{X})\}d\boldsymbol{X} \\
&= \underset{D\in\mathcal{D}}{\operatorname{argmin}} E_q\left[\frac{p(\boldsymbol{X})}{q(\boldsymbol{X})}\frac{Y}{P(A|\boldsymbol{X})}1\{A \neq D(\boldsymbol{X})\}\right] \\
&= \underset{D\in\mathcal{D}}{\operatorname{argmin}} E_q\left[\frac{\theta(\boldsymbol{X})Y}{P(A|\boldsymbol{X})}1\{A \neq D(\boldsymbol{X})\}\right].
\end{aligned}$$

Proof of Lemma 4.2

Let r_0 and r_1 be the sample proportions of $Y = 0$ and $Y = 1$, respectively. Then, using Bayes rule, we have

$$\begin{aligned} q(\boldsymbol{X}, A) &= r_0 P(\boldsymbol{X}, A|Y=0) + r_1 P(\boldsymbol{X}, A|Y=1) \\ &= \frac{r_0 p(\boldsymbol{X}, A, Y=0)}{P(Y=0)} + \frac{r_1 p(\boldsymbol{X}, A, Y=1)}{P(Y=1)} \\ &= \frac{r_0 P(Y=0|\boldsymbol{X}, A) p(\boldsymbol{X}, A)}{P(Y=0)} + \frac{r_1 P(Y=1|\boldsymbol{X}, A) p(\boldsymbol{X}, A)}{P(Y=1)} \\ &= P(A|\boldsymbol{X}) p(\boldsymbol{X}) \left[\frac{r_0 P(Y=0|\boldsymbol{X}, A)}{P(Y=0)} + \frac{r_1 P(Y=1|\boldsymbol{X}, A)}{P(Y=1)} \right]. \end{aligned}$$

Summing across $\mathcal{A}$, we obtain

$$q(\boldsymbol{X}) = \sum_{a \in \{-1,1\}} P(A=a|\boldsymbol{X}) p(\boldsymbol{X}) \left[\frac{r_0 P(Y=0|\boldsymbol{X}, A=a)}{P(Y=0)} + \frac{r_1 P(Y=1|\boldsymbol{X}, A=a)}{P(Y=1)} \right].$$

Finally, we see that

$$\begin{aligned} \theta(\boldsymbol{X}) &= \left[\frac{q(\boldsymbol{X})}{p(\boldsymbol{X})} \right]^{-1} \\ &= \left\{ \sum_{a \in \{-1,1\}} P(A=a|\boldsymbol{X}) \left[\frac{r_0 P(Y=0|\boldsymbol{X}, A=a)}{P(Y=0)} + \frac{r_1 P(Y=1|\boldsymbol{X}, A=a)}{P(Y=1)} \right] \right\}^{-1}. \end{aligned}$$

Proof of Theorem 4.1

This proof follows from Lemma 4.1 and results from Lin (2002). Recall that $\psi(u, v) = \max\{1 - \text{sign}(u)v, 0\}$. Minimizing the risk, $\mathcal{R}_\psi(f)$ is equivalent to minimizing the conditional risk,

$$\mathcal{R}_\psi(f, \boldsymbol{x}) = E\left[\widehat{\theta}(\boldsymbol{X}) \frac{|Y|}{P(A|\boldsymbol{X})} \psi\{Y, Af(\boldsymbol{X})\} \Big| \boldsymbol{X} = \boldsymbol{x} \right],$$

for every fixed $\boldsymbol{x} \in \mathcal{X}$. Let $Y^+ = Y1\{Y \geq 0\}$ and $Y^- = Y1\{Y < 0\}$. By the law of total expectation,

$$\begin{aligned}
\mathcal{R}_\psi(f, \boldsymbol{x}) &= E\left[\widehat{\theta}(\boldsymbol{X})|Y|\, \psi\{Y, f(\boldsymbol{X})\}\middle|\boldsymbol{X} = \boldsymbol{x}, A = 1\right] \\
&\quad + E\left[\widehat{\theta}(\boldsymbol{X})|Y|\, \psi\{Y, -f(\boldsymbol{X})\}\middle|\boldsymbol{X} = \boldsymbol{x}, A = -1\right] \\
&= \widehat{\theta}(\boldsymbol{X}) E\left[Y^+ \max\{1 - f(\boldsymbol{X}), 0\} - Y^- \max\{1 + f(\boldsymbol{X}), 0\}\middle|\boldsymbol{X} = \boldsymbol{x}, A = 1\right] \\
&\quad + \widehat{\theta}(\boldsymbol{X}) E\left[Y^+ \max\{1 + f(\boldsymbol{X}), 0\} - Y^- \max\{1 - f(\boldsymbol{X}), 0\}\middle|\boldsymbol{X} = \boldsymbol{x}, A = -1\right].
\end{aligned}$$

Next, note that $\mathcal{R}_\psi\{\text{sign}(f), \boldsymbol{x}\} < \mathcal{R}_\psi(f, \boldsymbol{x})$ whenever $f(\boldsymbol{x}) \notin [-1, 1]$. For example, when $f(\boldsymbol{x}) < -1$, the conditional risk reduces to

$$\widehat{\theta}(\boldsymbol{x})[1 - f(\boldsymbol{x})]\left\{E\left[Y^+\middle|\boldsymbol{X} = \boldsymbol{x}, A = 1\right] - E\left[Y^-\middle|\boldsymbol{X} = \boldsymbol{x}, A = -1\right]\right\},$$

which is monotonically increasing as $f(\boldsymbol{x}) \to -\infty$. A similar argument is made for when $f(\boldsymbol{x}) > 1$. Thus, we restrict our search to $f(\boldsymbol{x}) \in [-1, 1]$. Then,

$$\begin{aligned}
\mathcal{R}_\psi(f, \boldsymbol{x}) &\propto E\left[Y^+ - Y^-\middle|\boldsymbol{X} = \boldsymbol{x}, A = 1\right] + E\left[Y^+ - Y^-\middle|\boldsymbol{X} = \boldsymbol{x}, A = -1\right] \\
&\quad + f(\boldsymbol{X})\left\{-E\left[Y^+ - Y^-\middle|\boldsymbol{X} = \boldsymbol{x}, A = 1\right] + E\left[Y^+ + Y^-\middle|\boldsymbol{X} = \boldsymbol{x}, A = -1\right]\right\} \\
&= E\left[|Y|\middle|\boldsymbol{X} = \boldsymbol{x}, A = 1\right] + E\left[|Y|\middle|\boldsymbol{X} = \boldsymbol{x}, A = -1\right] \\
&\quad + f(\boldsymbol{X})\left\{E\left[Y\middle|\boldsymbol{X} = \boldsymbol{x}, A = -1\right] - E\left[Y\middle|\boldsymbol{X} = \boldsymbol{x}, A = 1\right]\right\}.
\end{aligned}$$

If $f^*(\boldsymbol{x})$ minimizes the conditional risk, then $f^*(x)$ must have the sign opposite of the expression $E\left[Y\middle|\boldsymbol{X} = \boldsymbol{x}, A = -1\right] - E\left[Y\middle|\boldsymbol{X} = \boldsymbol{x}, A = 1\right]$, and thus $D_0(\boldsymbol{X}) = \text{sign}\{f^*(\boldsymbol{X})\}$

Proof of Theorem 4.2

Define the loss function under ψ-loss to be

$$L_\psi(f) = \frac{\widehat{\theta}(\boldsymbol{X})|Y|}{P(A|\boldsymbol{X})}\psi\{Y, Af(\boldsymbol{X})\}.$$

For any $f \in \overline{F}$,

$$\mathbb{P}_n L_\psi(\widehat{f}_n^*) + \lambda_n ||\widehat{f}_n^*||^2 \leq \mathbb{P}_n L_\psi(f) + \lambda_n ||f||^2.$$

In particular, if we choose $f = 0$ and large enough n,

$$\begin{aligned} \mathbb{P}_n L_\psi(\widehat{f}_n^*) + \lambda_n ||\widehat{f}_n^*||^2 &\leq \mathbb{P}_n L_\psi(0) + \lambda_n ||0||^2 \\ &= \mathbb{P}\left\{\frac{\widehat{\theta}(\boldsymbol{X})|Y|}{P(A|\boldsymbol{X})}\right\} \\ &\leq \pi_0^{-1} M < \infty \end{aligned}$$

Because $\mathbb{P}_n L_\psi(\widehat{f}_n^*) \geq 0$, $\lambda_n ||\widehat{f}_n^*||^2$ is bounded by $\pi_0^{-1} M$. Next, consider that

$$\mathbb{P}_n L_\psi(\widehat{f}_n^*) \leq \mathbb{P}_n L_\psi(\widehat{f}_n^*) + \lambda_n ||\widehat{f}_n^*||^2 \leq \mathbb{P}_n L_\psi(f) + \lambda_n ||f||^2,$$

and taking the lim sup yields the following inequality.

$$\limsup_{n\to\infty} \mathbb{P}_n L_\psi(\widehat{f}_n^*) \leq \mathbb{P} L_\psi(f^*) + o_P(\lambda_n) \leq \mathbb{P} L_\psi(\widehat{f}_n^*) + o_P(\lambda_n)$$

Thus, it suffices to show that $\mathbb{P}_n L_\psi(\widehat{f}_n^*) - \mathbb{P} L_\psi(\widehat{f}_n^*) \to_P 0$. $\lambda_n ||\widehat{f}_n^*||^2$ is bounded which implies that $\{\sqrt{\lambda_n} f : ||\sqrt{\lambda_n} f|| \leq \sqrt{\pi_0^{-1} M}\}$ is contained in a Donsker class. $\psi(u, v)$ is Lipschitz continuous with respect to v. Therefore, $L_\psi(f)$ is Lipschitz continuous with respect to f, which further implies that $\{\sqrt{\lambda_n} L_\psi(f) : ||\sqrt{\lambda_n} f|| \leq \sqrt{\pi_0^{-1} M}\}$ is also Donsker. We now have that $\sqrt{n\lambda_n}\{\mathbb{P}_n - \mathbb{P}\} L_\psi(\widehat{f}_n^*) = O_p(1)$ and therefore $\{\mathbb{P}_n - \mathbb{P}\} L_\psi(\widehat{f}_n^*) = o_P(q)$. Thus,

$|\mathcal{R}_\psi(f^*) - \mathcal{R}_\psi(\widehat{f}_n^*)| = o_P(1)$. Furthermore, whenever $f_0^* \in \overline{\mathcal{F}}$, $f_0^* = f^*$, and

$$|\mathcal{R}(\widehat{f}_n^*) - \mathcal{R}(f_0)| \leq |\mathcal{R}_\psi(\widehat{f}_n^*) - \mathcal{R}_\psi(f_0^*)| = o_P(1),$$

where the first inequality holds from Bartlett et al. (2006)

BIBLIOGRAPHY

Adams, A. L., Black, M. H., Zhang, J. L., Shi, J. M., and Jacobsen, S. J. (2014). Proton-pump inhibitor use and hip fractures in men: a population-based case-control study. *Annals of Epidemiology*, 24(4):286–290.

Ahmad, A. and Dey, L. (2007). A k-mean clustering algorithm for mixed numeric and categorical data. *Data & Knowledge Engineering*, 63(2):503–527.

American Diabetes Association (2014). Diagnosis and classification of diabetes mellitus. *Diabetes Care*, 37(Supplement 1):S81–S90.

Anderson, J. W., Baird, P., Davis, R. H., Ferreri, S., Knudtson, M., Koraym, A., Waters, V., and Williams, C. L. (2009). Health benefits of dietary fiber. *Nutrition Reviews*, 67(4):188–205.

Anderson, J. W., Smith, B. M., and Gustafson, N. J. (1994). Health benefits and practical aspects of high-fiber diets. *The American Journal of Clinical Nutrition*, 59(5):1242S–1247S.

Armenian, H. K. (2009). *The case-control method: design and applications*, volume 38. Oxford University Press.

Armstrong, E. J., Chen, D. C., Westin, G. G., Singh, S., McCoach, C. E., Bang, H., Yeo, K.-K., Anderson, D., Amsterdam, E. A., and Laird, J. R. (2014). Adherence to guideline-recommended therapy is associated with decreased major adverse cardiovascular events and major adverse limb events among patients with peripheral arterial disease. *Journal of the American Heart Association*, 3(2):e000697.

Ashley, E. A. (2015). The precision medicine initiative: a new national effort. *Journal of the American Medical Association*, 313(21):2119–2120.

Athey, S. and Wager, S. (2017). Efficient policy learning. `https://arxiv.org/abs/1702.02896`.

Bair, E. (2013). Semi-supervised clustering methods. *Wiley Interdisciplinary Reviews: Computational Statistics*, 5(5):349–361.

Bair, E. and Tibshirani, R. (2004). Semi-supervised methods to predict patient survival from gene expression data. *PLoS Biology*, 2(4):e108.

Banfield, J. D. and Raftery, A. E. (1993). Model-based Gaussian and non-Gaussian clustering. *Biometrics*, pages 803–821.

Bartlett, P. L., Jordan, M. I., and McAuliffe, J. D. (2006). Convexity, classification, and risk bounds. *Journal of the American Statistical Association*, 101(473):138–156.

Bergman, R. N., Ider, Y. Z., Bowden, C. R., and Cobelli, C. (1979). Quantitative estimation of insulin sensitivity. *American Journal of Physiology-Endocrinology And Metabolism*, 236(6):E667.

Bleich, S. N., Vercammen, K. A., Zatz, L. Y., Frelier, J. M., Ebbeling, C. B., and Peeters, A. (2017). Interventions to prevent global childhood overweight and obesity: A systematic review. *The Lancet Diabetes & Endocrinology*, 6(4).

Boucher-Berry, C., Parton, E. A., and Alemzadeh, R. (2016). Excess weight gain during insulin pump therapy is associated with higher basal insulin doses. *Journal of Diabetes & Metabolic Disorders*, 15(1):47.

Breiman, L. (2001). Random forests. *Machine learning*, 45(1):5–32.

Breslow, N. and Day, N. (1980). Statistical methods in cancer research: the analysis of case–control studies. *IARC Sci Ppub*, 32:5–338.

Breslow, N. E. (1996). Statistics in epidemiology: the case-control study. *Journal of the American Statistical Association*, 91(433):14–28.

Brock, G., Pihur, V., Datta, S., Datta, S., et al. (2011). clValid, an R package for cluster validation. *Journal of Statistical Software (Brock et al., March 2008)*.

Burton, H., Sagoo, G. S., Pharoah, P., and Zimmern, R. L. (2012). Time to revisit Geoffrey Rose: strategies for prevention in the genomic era? *Italian Journal of Public Health*, 9(4).

Cambou, J. P., Aboyans, V., Constans, J., Lacroix, P., Dentans, C., and Bura, A. (2010). Characteristics and outcome of patients hospitalised for lower extremity peripheral artery disease in France: the COPART Registry. *European Journal of Vascular and Endovascular Surgery*, 39(5):577–585.

Chakraborty, B. and Murphy, S. A. (2014). Dynamic treatment regimes. *Annual Review of Statistics and its Application*, 1:447–464.

Charrad, M., Ghazzali, N., Boiteau, V., and Niknafs, A. (2014a). NbClust: An R package for determining the relevant number of clusters in a data set. *Journal of Statistical Software*, 61(6):1–36.

Charrad, M., Ghazzali, N., Boiteau, V., Niknafs, A., and Charrad, M. M. (2014b). Package 'NbClust'. *Journal of statistical software*, 61:1–36.

Chen, J., Fu, H., He, X., Kosorok, M. R., and Liu, Y. (2018). Estimating individualized treatment rules for ordinal treatments. *Biometrics*, 74(3):924–933.

Chiu, H.-T., Hubbard, B. K., Shah, A. N., Eide, J., Fredenburg, R. A., Walsh, C. T., and Khosla, C. (2001). Molecular cloning and sequence analysis of the complestatin biosynthetic gene cluster. *Proceedings of the National Academy of Sciences*, 98(15):8548–8553.

Collins, F. S. and Varmus, H. (2015). A new initiative on precision medicine. *New England Journal of Medicine*, 372(9):793–795.

Corbin, K. D., Driscoll, K. A., Pratley, R. E., Smith, S. R., Maahs, D. M., Mayer-Davis, E. J., for Type 1 Diabetes, A. C., and (ACT1ON), O. N. (2018). Obesity in type 1 diabetes: pathophysiology, clinical impact, and mechanisms. *Endocrine Reviews*, 39(5):629–663.

Cortes, C. and Vapnik, V. (1995). Support-vector networks. *Machine learning*, 20(3):273–297.

Deliu, M., Sperrin, M., Belgrave, D., and Custovic, A. (2016). Identification of asthma subtypes using clustering methodologies. *Pulmonary Therapy*, 2(1):19–41.

Dietterich, T. G. and Bakiri, G. (1994). Solving multiclass learning problems via error-correcting output codes. *Journal of Artificial Intelligence Research*, 2:263–286.

Dormandy, J. A. (2000). Management of peripheral arterial disease (PAD). TASC working group. TransAtlantic Inter-Society Consensus (TASC). *Journal of Vascular Surgery*, 31:S1–S296.

Driscoll, K. A., Corbin, K. D., Maahs, D. M., Pratley, R., Bishop, F. K., Kahkoska, A., Hood, K. K., Mayer-Davis, E., et al. (2017). Biopsychosocial aspects of weight management in type 1 diabetes: a review and next steps. *Current Diabetes Reports*, 17(8):58.

DuBose, S. N., Hermann, J. M., Tamborlane, W. V., Beck, R. W., Dost, A., DiMeglio, L. A., Schwab, K. O., Holl, R. W., Hofer, S. E., Maahs, D. M., et al. (2015). Obesity in youth with type 1 diabetes in Germany, Austria, and the United States. *The Journal of Pediatrics*, 167(3):627–632.

Dunn, J. C. (1974). Well-separated clusters and optimal fuzzy partitions. *Journal of Cybernetics*, 4(1):95–104.

Fleiss, J. L. (1989). A critique of recent research on the two-treatment crossover design. *Controlled Clinical Trials*, 10(3):237–243.

Foster, N. C., Beck, R. W., Miller, K. M., Clements, M. A., Rickels, M. R., DiMeglio, L. A., Maahs, D. M., Tamborlane, W. V., Bergenstal, R., Smith, E., et al. (2019). State of type 1 diabetes management and outcomes from the T1D exchange in 2016–2018. *Diabetes Technology & Therapeutics*.

Friedman, J., Hastie, T., and Tibshirani, R. (2001). *The elements of statistical learning*, volume 1. Springer series in statistics New York.

Friedman, J., Hastie, T., and Tibshirani, R. (2010). Regularization paths for generalized linear models via coordinate descent. *Journal of Statistical Software*, 33(1):1–22.

Friedman, J. H. (1991). Multivariate adaptive regression splines. *The Annals of Statistics*, 19(1):1–67.

Fröhlich-Reiterer, E. E., Rosenbauer, J., Bechtold-Dalla Pozza, S., Hofer, S. E., Schober, E., Holl, R. W., Group, D.-W. S., mellitus, G. B. C. N. D., Obesity, et al. (2014). Predictors of increasing BMI during the course of diabetes in children and adolescents with type 1 diabetes: data from the German/Austrian DPV multicentre survey. *Archives of Disease in Childhood*, 99(8):738–743.

Fu, H., Zhou, J., and Faries, D. E. (2016). Estimating optimal treatment regimes via subgroup identification in randomized control trials and observational studies. *Statistics in Medicine*, 35(19):3285–3302.

Garg, S. K., Weinzimer, S. A., Tamborlane, W. V., Buckingham, B. A., Bode, B. W., Bailey, T. S., Brazg, R. L., Ilany, J., Slover, R. H., Anderson, S. M., et al. (2017). Glucose outcomes with the in-home use of a hybrid closed-loop insulin delivery system in adolescents and adults with type 1 diabetes. *Diabetes Technology & Therapeutics*, 19(3):155–163.

Gaynor, S. and Bair, E. (2017). Identification of relevant subtypes via preweighted sparse clustering. *Computational Statistics & Data Analysis*, 116:139–154.

Genolini, C. and Falissard, B. (2010). KmL: k-means for longitudinal data. *Computational Statistics*, 25(2):317–328.

Gerald R. Fowkes, F., Housley, E., Riemersma, R. A., Macintyre, C. C., Cawood, E. H., Prescott, R. J., and Ruckley, C. V. (1992). Smoking, lipids, glucose intolerance, and blood pressure as risk factors for peripheral atherosclerosis compared with ischemic heart disease in the Edinburgh Artery Study. *American Journal of Epidemiology*, 135(4):331–340.

Gerhard-Herman, M. D., Gornik, H. L., Barrett, C., Barshes, N. R., Corriere, M. A., Drachman, D. E., Fleisher, L. A., Fowkes, F. G. R., Hamburg, N. M., Kinlay, S., et al. (2017). 2016 AHA/ACC guideline on the management of patients with lower extremity peripheral artery disease: a report of the American College of Cardiology/American Heart Association Task Force on Clinical Practice Guidelines. *Journal of the American College of Cardiology*, 69(11):e71–e126.

Glicksberg, B. S., Johnson, K. W., and Dudley, J. T. (2018). The next generation of precision medicine: observational studies, electronic health records, biobanks and continuous monitoring. *Human Molecular Genetics*, 27(R1):R56–R62.

Haendel, M. A., Chute, C. G., and Robinson, P. N. (2018). Classification, ontology, and precision medicine. *New England Journal of Medicine*, 379(15):1452–1462.

Halliday, T. M., Liu, S. V., Moore, L. B., Hedrick, V. E., and Davy, B. M. (2018). Adolescents perceive a low added sugar adequate fiber diet to be more satiating and equally palatable compared to a high added sugar low fiber diet in a randomized-crossover design controlled feeding pilot trial. *Eating Behaviors*, 30:9–15.

Hamman, R. F., Bell, R. A., Dabelea, D., D'agostino, R. B., Dolan, L., Imperatore, G., Lawrence, J. M., Linder, B., Marcovina, S. M., Mayer-Davis, E. J., et al. (2014). The search for diabetes in youth study: rationale, findings, and future directions. *Diabetes Care*, 37(12):3336–3344.

Handl, J., Knowles, J., and Kell, D. B. (2005). Computational cluster validation in post-genomic data analysis. *Bioinformatics*, 21(15):3201–3212.

Hartigan, J. A. and Wong, M. A. (1979). Algorithm as 136: A k-means clustering algorithm. *Journal of the Royal Statistical Society. Series C (Applied Statistics)*, 28(1):100–108.

Hernán, M. A. and Robins, J. M. (2018). *Causal Inference*. Boca Raton: Chapman & Hall/CRC. Forthcoming.

Hiatt, W. R. (2001). Medical treatment of peripheral arterial disease and claudication. *New England Journal of Medicine*, 344(21):1608–1621.

Hirsch, A. T., Criqui, M. H., Treat-Jacobson, D., Regensteiner, J. G., Creager, M. A., Olin, J. W., Krook, S. H., Hunninghake, D. B., Comerota, A. J., Walsh, M. E., et al. (2001). Peripheral arterial disease detection, awareness, and treatment in primary care. *JAMA*, 286(11):1317–1324.

Hirsch, A. T., Hartman, L., Town, R. J., and Virnig, B. A. (2008). National health care costs of peripheral arterial disease in the medicare population. *Vascular Medicine*, 13(3):209–215.

Holloway, S. T., Laber, E. B., Linn, K. A., Zhang, B., Davidian, M., and Tsiatis, A. A. (2018). *DynTxRegime: Methods for Estimating Optimal Dynamic Treatment Regimes*. R package version 3.2.

Hood, K. K., Peterson, C. M., Rohan, J. M., and Drotar, D. (2009). Association between adherence and glycemic control in pediatric type 1 diabetes: a meta-analysis. *Pediatrics*, 124(6):e1171–e1179.

Hsu, C.-C. and Huang, Y.-P. (2008). Incremental clustering of mixed data based on distance hierarchy. *Expert Systems with Applications*, 35(3):1177–1185.

Hubert, L. and Arabie, P. (1985). Comparing partitions. *Journal of Classification*, 2(1):193–218.

Ishwaran, H. and Kogalur, U. (2007). Random survival forests for R. *R News*, 7(2):25–31.

Ishwaran, H., Kogalur, U., Blackstone, E., and Lauer, M. (2008). Random survival forests. *Ann. Appl. Statist.*, 2(3):841–860.

Jang, A. S., Kwon, H.-S., Cho, Y. S., Bae, Y. J., Kim, T. B., Park, J. S., Park, S. W., Uh, S.-T., Choi, J.-S., Kim, Y.-H., et al. (2013). Identification of subtypes of refractory asthma in Korean patients by cluster analysis. *Lung*, 191(1):87–93.

Kahkoska, A. R., Shay, C. M., Crandell, J., Dabelea, D., Imperatore, G., Lawrence, J. M., Liese, A. D., Pihoker, C., Reboussin, B. A., Agarwal, S., et al. (2018). Association of race and ethnicity with glycemic control and hemoglobin A1c levels in youth with type 1 diabetes. *JAMA Network Open*, 1(5):e181851–e181851.

Kallus, N. (2018). Balanced policy evaluation and learning. In *Advances in Neural Information Processing Systems*, pages 8908–8919.

Kannel, W. B. (1973). The Framingham Study: cigarettes and the development of intermittent claudication. *Geriatrics*, 28:61–68.

Keavney, B., Palmer, A., Parish, S., Clark, S., Youngman, L., Danesh, J., McKenzie, C., Delépine, M., Lathrop, M., Peto, R., et al. (2004). Lipid-related genes and myocardial infarction in 4685 cases and 3460 controls: discrepancies between genotype, blood lipid concentrations, and coronary disease risk. *International Journal of Epidemiology*, 33(5):1002–1013.

Keogh, R. H. and Cox, D. R. (2014). *Case-control studies*, volume 4. Cambridge University Press.

Khachaturian, A. S., Corcoran, C. D., Mayer, L. S., Zandi, P. P., and Breitner, J. C. (2004). Apolipoprotein E ϵ4 count affects age at onset of Alzheimer disease, but not lifetime susceptibility: the Cache County Study. *Archives of general psychiatry*, 61(5):518–524.

Kimeldorf, G. S. and Wahba, G. (1970). A correspondence between Bayesian estimation on stochastic processes and smoothing by splines. *The Annals of Mathematical Statistics*, 41(2):495–502.

Kipping, R. R., Jago, R., and Lawlor, D. A. (2008). Obesity in children. part 1: Epidemiology, measurement, risk factors, and screening. *BMJ: British Medical Journal*, 337:a1824.

Koestler, D. C., Christensen, B. C., Marsit, C. J., Kelsey, K. T., and Houseman, E. A. (2013). Recursively partitioned mixture model clustering of DNA methylation data using biologically informed correlation structures. *Statistical Applications in Genetics and Molecular Biology*, 12(2):225–240.

Kosorok, M. R. and Moodie, E. E. (2015). *Adaptive Treatment Strategies in Practice: Planning Trials and Analyzing Data for Personalized Medicine*, volume 21. SIAM.

Kulasekera, K. B. and Siriwardhana, C. (2018). Multi-response based personalized treatment selection with data from crossover designs for multiple treatments. `https://louisville.edu/sphis/departments/bioinformatics-biostatistics/pdfs/BST2018-01.pdf`.

Laber, E. and Zhao, Y. (2015). Tree-based methods for individualized treatment regimes. *Biometrika*, 102(3):501–514.

Laber, E. B., Lizotte, D. J., Qian, M., Pelham, W. E., and Murphy, S. A. (2014). Dynamic treatment regimes: Technical challenges and applications. *Electronic Journal of Statistics*, 8(1):1225.

Lavori, P. W. and Dawson, R. (2014). Introduction to dynamic treatment strategies and sequential multiple assignment randomization. *Clinical Trials*, 11(4):393–399.

Lee, Y., Lin, Y., and Wahba, G. (2004). Multicategory support vector machines: Theory and application to the classification of microarray data and satellite radiance data. *Journal of the American Statistical Association*, 99(465):67–81.

Liang, M., Ye, T., and Fu, H. (2018). Estimating individualized optimal combination therapies through outcome weighted deep learning algorithms. *Statistics in Medicine*, 37(27):3869–3886.

Liaw, A. and Wiener, M. (2002). Classification and regression by randomforest. *R News*, 2(3):18–22.

Lin, Y. (2002). Support vector machines and the Bayes rule in classification. *Data Mining and Knowledge Discovery*, 6(3):259–275.

Liu, L. L., Lawrence, J. M., Davis, C., Liese, A. D., Pettitt, D. J., Pihoker, C., Dabelea, D., Hamman, R., Waitzfelder, B., Kahn, H. S., et al. (2010). Prevalence of overweight and obesity in youth with diabetes in USA: the SEARCH for Diabetes in Youth study. *Pediatric Diabetes*, 11(1):4–11.

Lötvall, J., Akdis, C. A., Bacharier, L. B., Bjermer, L., Casale, T. B., Custovic, A., Lemanske Jr, R. F., Wardlaw, A. J., Wenzel, S. E., and Greenberger, P. A. (2011). Asthma endotypes: a new approach to classification of disease entities within the asthma syndrome. *Journal of Allergy and Clinical Immunology*, 127(2):355–360.

Lowe, L. A., Simpson, A., Woodcock, A., Morris, J., Murray, C. S., and Custovic, A. (2005). Wheeze phenotypes and lung function in preschool children. *American Journal of Respiratory and Critical Care Medicine*, 171(3):231–237.

Machin, D. and Fayers, P. M. (2010). *Randomized clinical trials: design, practice and reporting*. John Wiley & Sons.

Maechler, M., Rousseeuw, P., Struyf, A., Hubert, M., and Hornik, K. (2017). *cluster: Cluster Analysis Basics and Extensions*. R package version 2.0.6 — For new features, see the 'Changelog' file (in the package source).

Manyanga, T., Sellers, E. A., Wicklow, B. A., Doupe, M., and Fransoo, R. (2016). Is the change in body mass index among children newly diagnosed with type 1 diabetes mellitus associated with obesity at transition from pediatric to adult care? *Pediatric Diabetes*, 17(8):599–607.

Marlett, J. A., McBurney, M. I., and Slavin, J. L. (2002). Position of the American Dietetic Association: health implications of dietary fiber. *Journal of the American Dietetic Association*, 102(7):993–1000.

Mehta, S. N., Andersen, H. U., Abrahamson, M. J., Wolpert, H. A., Hommel, E. E., McMullen, W., and Ridderstråle, M. (2017). Changes in HbA1c and weight following transition to continuous subcutaneous insulin infusion therapy in adults with type 1 diabetes. *Journal of Diabetes Science and Technology*, 11(1):83–86.

Miller, K. M., Foster, N. C., Beck, R. W., Bergenstal, R. M., DuBose, S. N., DiMeglio, L. A., Maahs, D. M., and Tamborlane, W. V. (2015). Current state of type 1 diabetes treatment in the us: updated data from the T1D exchange clinic registry. *Diabetes Care*, 38(6):971–978.

Minges, K. E., Whittemore, R., Chao, A. M., Jefferson, V., Murphy, K. M., and Grey, M. (2016). Clinical, psychosocial, and demographic factors are associated with overweight and obesity in early adolescent girls with type 1 diabetes. *The Diabetes Educator*, 42(5):538–548.

Minges, K. E., Whittemore, R., Weinzimer, S. A., Irwin, M. L., Redeker, N. S., and Grey, M. (2017). Correlates of overweight and obesity in 5529 adolescents with type 1 diabetes: The T1D exchange clinic registry. *Diabetes Research and Clinical Practice*, 126:68–78.

Moodie, E. E., Chakraborty, B., and Kramer, M. S. (2012). Q-learning for estimating optimal dynamic treatment rules from observational data. *Canadian Journal of Statistics*, 40(4):629–645.

Moodie, E. E., Richardson, T. S., and Stephens, D. A. (2007). Demystifying optimal dynamic treatment regimes. *Biometrics*, 63(2):447–455.

Mortensen, M. B., Fuster, V., Muntendam, P., Mehran, R., Baber, U., Sartori, S., and Falk, E. (2016). A simple disease-guided approach to personalize ACC/AHA-recommended statin allocation in elderly people: the BioImage Study. *Journal of the American College of Cardiology*, 68(9):881–891.

Mozaffarian, D., Benjamin, E. J., Go, A. S., Arnett, D. K., Blaha, M. J., Cushman, M., De Ferranti, S., Després, J.-P., Fullerton, H. J., Howard, V. J., et al. (2015). Executive summary: heart disease and stroke statistics—2015 update: a report from the American Heart Association. *Circulation*, 131(4):434–441.

Muntner, P., Wildman, R. P., Reynolds, K., DeSalvo, K. B., Chen, J., and Fonseca, V. (2005). Relationship between HbA1c level and peripheral arterial disease. *Diabetes Care*, 28(8):1981–1987.

Navas-Acien, A., Selvin, E., Sharrett, A. R., Calderon-Aranda, E., Silbergeld, E., and Guallar, E. (2004). Lead, cadmium, smoking, and increased risk of peripheral arterial disease. *Circulation*, 109(25):3196–3201.

Ogden, C. L., Carroll, M. D., Kit, B. K., and Flegal, K. M. (2014). Prevalence of childhood and adult obesity in the United States, 2011-2012. *Journal of the American Medical Association*, 311(8):806–814.

Olson, J. E., Bielinski, S. J., Ryu, E., Winkler, E., Takahashi, P. Y., Pathak, J., and Cerhan, J. R. (2014). Biobanks and personalized medicine. *Clinical Genetics*, 86(1):50–55.

Orchard, T. J., Nathan, D. M., Zinman, B., Cleary, P., Brillon, D., Backlund, J.-Y. C., and Lachin, J. M. (2015). Association between 7 years of intensive treatment of type 1 diabetes and long-term mortality. *JAMA*, 313(1):45–53.

O'Reilly, G. A., Belcher, B. R., Davis, J. N., Martinez, L. T., Huh, J., Antunez-Castillo, L., Weigensberg, M., Goran, M. I., and Spruijt-Metz, D. (2015). Effects of high-sugar and high-fiber meals on physical activity behaviors in Latino and African American adolescents. *Obesity*, 23(9):1886–1894.

Palen, T. E., Price, D., Shetterly, S., and Wallace, K. B. (2012). Comparing virtual consults to traditional consults using an electronic health record: an observational case–control study. *BMC Medical Informatics and Decision Making*, 12(1):65.

Pańkowska, E., Szypowska, A., and Lipka, M. (2008). Basal insulin and total daily insulin dose in children with type 1 diabetes using insulin pumps. *Pediatric Diabetes*, 9(3pt1):208–213.

Park, H.-W., Song, W.-J., Kim, S.-H., Park, H.-K., Kim, S.-H., Kwon, Y. E., Kwon, H.-S., Kim, T.-B., Chang, Y.-S., Cho, Y.-S., et al. (2015). Classification and implementation of asthma phenotypes in elderly patients. *Annals of Allergy, Asthma & Immunology*, 114(1):18–22.

Parzen, E. (1962). On estimation of a probability density function and mode. *The Annals of Mathematical Statistics*, 33(3):1065–1076.

Petersen, M. L., Deeks, S. G., and van der Laan, M. J. (2007). Individualized treatment rules: Generating candidate clinical trials. *Statistics in Medicine*, 26(25):4578–4601.

Petitti, D. B., Klingensmith, G. J., Bell, R. A., Andrews, J. S., Dabelea, D., Imperatore, G., Marcovina, S., Pihoker, C., Standiford, D., Waitzfelder, B., et al. (2009). Glycemic control in youth with diabetes: the SEARCH for Diabetes in Youth study. *The Journal of Pediatrics*, 155(5):668–672.

Purnell, J. Q., Braffett, B. H., Zinman, B., Gubitosi-Klug, R. A., Sivitz, W., Bantle, J. P., Ziegler, G., Cleary, P. A., Brunzell, J. D., Group, D. R., et al. (2017). Impact of excessive weight gain on cardiovascular outcomes in type 1 diabetes: results from the diabetes control and complications trial/epidemiology of diabetes interventions and complications (DCCT/EDIC) study. *Diabetes Care*, 40(12):1756–1762.

Purnell, J. Q., Hokanson, J. E., Marcovina, S. M., Steffes, M. W., Cleary, P. A., and Brunzell, J. D. (1998). Effect of excessive weight gain with intensive therapy of type 1 diabetes on lipid levels and blood pressure: results from the DCCT. *JAMA*, 280(2):140–146.

Qian, M. and Murphy, S. A. (2011). Performance guarantees for individualized treatment rules. *Annals of Statistics*, 39(2):1180.

Qiu, C., Kivipelto, M., Agüero-Torres, H., Winblad, B., and Fratiglioni, L. (2004). Risk and protective effects of the APOE gene towards Alzheimer's disease in the Kungsholmen project: variation by age and sex. *Journal of Neurology, Neurosurgery & Psychiatry*, 75(6):828–833.

R Core Team (2017). *R: A Language and Environment for Statistical Computing*. R Foundation for Statistical Computing, Vienna, Austria.

Rosenblatt, M. (1956). Remarks on some nonparametric estimates of a density function. *The Annals of Mathematical Statistics*, pages 832–837.

Rössner, S., Von Zweigbergk, D., Öhlin, A., and Ryttig, K. (1987). Weight reduction with dietary fibre supplements: Results of two double-blind randomized studies. *Acta Medica Scandinavica*, 222(1):83–88.

Rousseeuw, P. J. (1987). Silhouettes: a graphical aid to the interpretation and validation of cluster analysis. *Journal of Computational and Applied Mathematics*, 20:53–65.

Rubin, D. B. (1978). Bayesian inference for causal effects: The role of randomization. *The Annals of Statistics*, 6(1):34–58.

Ryttig, K., Tellnes, G., Haegh, L., Bøe, E., and Fagerthun, H. (1989). A dietary fibre supplement and weight maintenance after weight reduction: A randomized, double-blind, placebo-controlled long-term trial. *International Journal of Obesity*, 13(2):165–171.

Selvin, E., Wattanakit, K., Steffes, M. W., Coresh, J., and Sharrett, A. R. (2006). HbA1c and peripheral arterial disease in diabetes: the Atherosclerosis Risk in Communities study. *Diabetes Care*, 29(4):877–882.

Silverman, B. W. (2018). *Density estimation for statistics and data analysis*. Routledge.

Slavin, J. L. (2005). Dietary fiber and body weight. *Nutrition*, 21(3):411–418.

Smith, G. D., Ebrahim, S., Lewis, S., Hansell, A. L., Palmer, L. J., and Burton, P. R. (2005). Genetic epidemiology and public health: hope, hype, and future prospects. *The Lancet*, 366(9495):1484–1498.

Song, R., Kosorok, M., Zeng, D., Zhao, Y., Laber, E., and Yuan, M. (2015). On sparse representation for optimal individualized treatment selection with penalized outcome weighted learning. *Stat; Bulletin of the Wisconsin Nurses Association*, 4(1):59–68.

Stekhoven, D. J. (2013). *missForest: Nonparametric Missing Value Imputation using Random Forest*. R package version 1.4.

Stekhoven, D. J. and Bühlmann, P. (2012). Missforest—non-parametric missing value imputation for mixed-type data. *Bioinformatics*, 28(1):112–118.

Tao, P. D. (2005). The DC (difference of convex functions) programming and DCA revisited with DC models of real world nonconvex optimization problems. *Annals of Operations Research*, 133(1-4):23–46.

Taveras, E. M., Gillman, M. W., Kleinman, K. P., Rich-Edwards, J. W., and Rifas-Shiman, S. L. (2013). Reducing racial/ethnic disparities in childhood obesity: The role of early life risk factors. *Journal of the American Medical Association Pediatrics*, 167(8):731–738.

Thompson, W. G., Holdman, N. R., Janzow, D. J., Slezak, J. M., Morris, K. L., and Zemel, M. B. (2005). Effect of energy-reduced diets high in dairy products and fiber on weight loss in obese adults. *Obesity Research*, 13(8):1344–1353.

Tucker, L. A. and Thomas, K. S. (2009). Increasing total fiber intake reduces risk of weight and fat gains in women. *The Journal of Nutrition*, 139(3):576–581.

Turner, J. R. (2010). *New drug development: An introduction to clinical trials*. Springer Science & Business Media.

US Department of Agriculture (2010). US Department of Health and Human Services. Dietary Guidelines for Americans.

Van Der Laan, M. J. (2008). Estimation based on case-control designs with known incidence probability.

Walsh, M. C., Trentham-Dietz, A., Newcomb, P. A., Gangnon, R., and Palta, M. (2012). Using propensity scores to reduce case-control selection bias. *Epidemiology (Cambridge, Mass.)*, 23(5):772.

Wang, Y. and Chen, H.-J. (2012). Use of percentiles and z-scores in anthropometry. In *Handbook of Anthropometry*, pages 29–48. Springer.

Wang, Y., Wu, P., Liu, Y., Weng, C., and Zeng, D. (2016). Learning optimal individualized treatment rules from electronic health record data. In *Healthcare Informatics (ICHI), 2016 IEEE International Conference on*, pages 65–71. IEEE.

Ward Jr, J. H. (1963). Hierarchical grouping to optimize an objective function. *Journal of the American Statistical Association*, 58(301):236–244.

Wattanakit, K., Folsom, A. R., Selvin, E., Weatherley, B. D., Pankow, J. S., Brancati, F. L., and Hirsch, A. T. (2005). Risk factors for peripheral arterial disease incidence in persons with diabetes: the Atherosclerosis Risk in Communities (ARIC) Study. *Atherosclerosis*, 180(2):389–397.

Wellek, S. and Blettner, M. (2012). On the proper use of the crossover design in clinical trials: Part 18 of a series on evaluation of scientific publications. *Deutsches Ärzteblatt International*, 109(15):276.

Wenzel, S. E. (2006). Asthma: defining of the persistent adult phenotypes. *The Lancet*, 368(9537):804–813.

Witten, D. M. and Tibshirani, R. (2010). A framework for feature selection in clustering. *Journal of the American Statistical Association*, 105(490):713–726.

Woo, K., Palmer, O. P., Weaver, F. A., Rowe, V. L., for Vascular Surgery Vascular Quality Initiative, S., et al. (2015). Use of completion imaging during infrainguinal bypass in the Vascular Quality Initiative. *Journal of Vascular Surgery*, 61(5):1258–1263.

Wu, J., Roy, J., and Stewart, W. F. (2010). Prediction modeling using ehr data: challenges, strategies, and a comparison of machine learning approaches. *Medical Care*, pages S106–S113.

Xu, Y., Yu, M., Zhao, Y.-Q., Li, Q., Wang, S., and Shao, J. (2015). Regularized outcome weighted subgroup identification for differential treatment effects. *Biometrics*, 71(3):645–653.

Yang, Y. J., Youn, J. H., and Bergman, R. N. (1987). Modified protocols improve insulin sensitivity estimation using the minimal model. *American Journal of Physiology-Endocrinology And Metabolism*, 253(6):E595–E602.

Yeung, K. Y., Haynor, D. R., and Ruzzo, W. L. (2001). Validating clustering for gene expression data. *Bioinformatics*, 17(4):309–318.

Zhang, B., Tsiatis, A. A., Davidian, M., Zhang, M., and Laber, E. (2012b). Estimating optimal treatment regimes from a classification perspective. *Stat; Bulletin of the Wisconsin Nurses Association*, 1(1):103–114.

Zhang, B., Tsiatis, A. A., Laber, E. B., and Davidian, M. (2012a). A robust method for estimating optimal treatment regimes. *Biometrics*, 68(4):1010–1018.

Zhao, Y. and Zeng, D. (2013). Recent development on statistical methods for personalized medicine discovery. *Frontiers of Medicine*, 7(1):102–110.

Zhao, Y., Zeng, D., Rush, A. J., and Kosorok, M. R. (2012). Estimating individualized treatment rules using outcome weighted learning. *Journal of the American Statistical Association*, 107(499):1106–1118.

Zhou, W., Liu, G., Thurston, S. W., Xu, L. L., Miller, D. P., Wain, J. C., Lynch, T. J., Su, L., and Christiani, D. C. (2002). Genetic polymorphisms in n-acetyltransferase-2 and microsomal epoxide hydrolase, cumulative cigarette smoking, and lung cancer. *Cancer Epidemiology and Prevention Biomarkers*, 11(1):15–21.

Zhou, X., Mayer-Hamblett, N., Khan, U., and Kosorok, M. R. (2017). Residual weighted learning for estimating individualized treatment rules. *Journal of the American Statistical Association*, 112(517):169–187.

Zhu, J., Rosset, S., Tibshirani, R., and Hastie, T. J. (2004). 1-norm support vector machines. In *Advances in Neural Information Processing Systems*, pages 49–56.

Zhu, R. (2017). *Reinforcement Learning Trees*. R package version 3.2.1.

Zhu, R., Zeng, D., and Kosorok, M. R. (2015). Reinforcement learning trees. *Journal of the American Statistical Association*, 110(512):1770–1784.